

2023-08-15

More than agriculture: analysing time-cumulative human impact on European land-cover of second half of the Holocene

Zapolska, A

<https://pearl.plymouth.ac.uk/handle/10026.1/21041>

10.1016/j.quascirev.2023.108227

Quaternary Science Reviews

Elsevier

All content in PEARL is protected by copyright law. Author manuscripts are made available in accordance with publisher policies. Please cite only the published version using the details provided on the item record or document. In the absence of an open licence (e.g. Creative Commons), permissions for further reuse of content should be sought from the publisher or author.

1 More than agriculture: analysing time-cumulative human impact on European land-
2 cover of second half of the Holocene

3 Authors:

4 Anhelina Zapolska¹, Maria Antonia Serge², Florence Mazier², Aurélien Quiquet³, Hans Renssen⁴, Mathieu
5 Vrac³, Ralph Fyfe⁵, Didier M. Roche^{1,3}

6
7 ¹ Earth and Climate Cluster, Faculty of Science, Vrije Universiteit Amsterdam, 1081 HV Amsterdam, the
8 Netherlands

9 ² Laboratoire Géographie de l'Environnement, UMR 5602, CNRS, Université de Toulouse-Jean Jaurès, 31058
10 Toulouse, France

11 ³ Laboratoire des Sciences du Climat et de l'Environnement, LSCE/IPSL, CEA-CNRS-UVSQ, Université Paris-
12 Saclay, 91190 Gif-sur-Yvette, France

13 ⁴ Department of Natural Sciences and Environmental Health, University of South-Eastern Norway, 3800 Bø,
14 Norway

15 ⁵ School of Geography, Earth and Environmental Sciences, University of Plymouth, PL4 8AA Plymouth, UK

16
17 Corresponding Author: zapolskaanhelina@gmail.com

18

19

20 Abstract:

21 Assessment of past anthropogenic modifications of land-cover dynamics is key to understanding the human
22 role in the Earth system. Recent advances in palaeoenvironmental sciences allow us to assess the long-term
23 impacts of anthropization on ecosystems, landscapes, and land-cover.

24 Our study aims to evaluate the role of human impact on European land-cover over the past 6000 years by
25 comparing two independent datasets. First, we use a dynamic vegetation model forced by debiased climate
26 model outputs. The climate model uses natural forcings only and therefore the computed vegetation
27 distribution is interpreted as the potential natural vegetation. Second, we use pollen-based reconstructions,
28 which intrinsically include anthropogenic influence. The discrepancies between the two datasets are attributed
29 to human activity and quantified in a form of a human pressure index (HPI).

30 Patterns of spatio-temporal evolution of the HPI agree with previously published data about the spread of
31 agriculture in Europe. In particular, both HPI and anthropogenic land-cover change (ALCC) scenarios indicate
32 a rapid increase of the human pressure around 1200-1700 BP, and a significant increase of agriculture-related
33 land-cover modifications by nearly 60% throughout the second half of the Holocene. However, initially high HPI
34 values (up to 70%) at 5700-6200 BP, which correlate with population estimates ($r = 0.75$, $p\text{-value} < 0.005$),
35 suggest high levels of anthropogenic land-cover transformations, introduced by earlier agricultural as well as
36 non-agricultural activities.

37 The results of our study suggest that vegetation cover of the Mid-Holocene substantially differed from the state
38 of potential natural vegetation (PNV) due to cumulative effect of early human alterations on the land-cover.

39 This challenges the hypothesis that vegetation in the Mid-Holocene was in a relatively natural state and
40 contributes valuable insights to the onset of agriculture as the start of the Anthropocene.

41

42 Keywords: anthropogenic land-cover change; climate-forced vegetation modelling; pollen-based
43 reconstructions; Europe

44

45 Highlights:

- 46 • This study quantifies European anthropogenic land cover changes using human pressure index (HPI)
- 47 • HPI shows 60% increase in anthropogenic land-cover modifications throughout the second half of the
48 Holocene
- 49 • Population estimates correlate with HPI and agree with previously published data on land use
- 50 • High HPI values in the Mid-Holocene suggest significant impact of early agricultural and pre-agricultural
51 human practices

52

53 1. Introduction

54 Numerous scholars, particularly within the geological community, mark the start of the Anthropocene by the
55 transition to fossil fuel burning, artificial radionuclides spread by the thermonuclear bomb tests or rapid
56 changes in the biosphere, which typically begin between the Industrial Revolution (ca. AD 1800) and the early
57 1950s (Bauer et al., 2021; Crutzen, 2002; Head et al., 2022a; Steffen et al., 2011; Waters et al., 2016;
58 Zalasiewicz et al., 2021). However, in recent years researchers propose to account for the emergence of
59 humanity as a force on Earth's landscape. Scholars in archaeological and palaeoecological communities argue
60 that humans begun substantially impacting the environment several thousands of years earlier than previously
61 suggested (Braje and Erlandson, 2013b; Ellis et al., 2021; Erlandson and Braje, 2013; Lightfoot and Cuthrell,
62 2015; Nikulina et al., 2022; Smith and Zeder, 2013). It is thus debatable whether Anthropocene's "golden
63 spike" should be marked by the appearance of anthropogenic soils (Certini and Scalenghe, 2011), onset of
64 agriculture (Ruddiman, 2013), late Pleistocene megafaunal extinctions (Braje and Erlandson, 2013a), or
65 defining the "Anthropocene" term should be omitted altogether and used as a flexible term instead (Edgeworth
66 et al., 2015; Ruddiman, 2018; Rull, 2017; Swindles et al., 2023). Moreover, other terminology was proposed to
67 define early hominin impact on the environment, such as the Palaeoanthropocene (Foley et al., 2013). To
68 address the challenges associated with formalizing the Anthropocene as a distinct epoch (subdivision of the
69 Geological Time Scale), recent studies suggest to define the Anthropocene as an ongoing event (Edwards et
70 al., 2022; Gibbard et al., 2022; Bauer et al., 2021) or episode (Head et al., 2022b), rather than an epoch. In any
71 case, in the light of the Anthropocene discussion, the history of anthropogenic impact on land-cover became a
72 key topic in palaeoenvironmental studies.

73 The role of land-cover modifications attributed to human activity over the Holocene is often quantified by
74 means of anthropogenic land-cover change (ALCC) models (HYDE 3.2: Goldewijk et al., 2017; KK10: Kaplan
75 et al., 2009; Pongratz et al., 2008). While their reliability is largely limited by a number of factors, such as not
76 explicitly accounting for effects of Holocene climate or geomorphic change and variability, and uncertainties in
77 the underlying data, ALCC models are currently the only available method to produce spatially- and temporally-
78 continuous data of numerically expressed human-environment interactions (Kaplan et al., 2017). These models
79 are based on historical human population density estimates, the land needed to sustain that population, and its
80 suitability, determined by climate and soil properties (Kaplan et al., 2009; Pirzamanbein and Lindström, 2022).

81 However, ALCC models, such as KK10 or HYDE 3.2, do not yet incorporate archaeological and
82 palaeoecological proxy data or historical descriptions of past land use (Trondman et al., 2015). Several
83 approaches have been developed to estimate past ALCCs to assess their possible effects on past land-cover
84 (Ramankutty and Foley, 1999; Olofsson and Hickler, 2008; Pongratz et al., 2008, 2010; Kaplan et al., 2009,
85 2011; Lemmen, 2009; Goldewijk et al., 2011). While existing ALCC scenarios (Goldewijk et al., 2017a; Kaplan
86 et al., 2009; Pongratz et al., 2008) significantly differ from each other (Gaillard et al., 2010; Kaplan et al., 2017),
87 they all tend to represent anthropogenic impact centred around agricultural activities. For example, multiple
88 studies focus on their representation of the onset and adoption of agriculture in different ALCC scenarios
89 (Smith et al., 2016; Stephens et al., 2019; Stocker et al., 2011; Vavrus et al., 2022). KK10 in particular,
90 features deforestation for crop cultivation and pastures to quantify human influence on land-cover (Kaplan et
91 al., 2009). However, deforestation by humans is not limited to agricultural purposes. Harrison et al. (2020), and
92 even Kaplan et al. (2017) themselves highlighted the need for inclusion of non-agricultural activities in the
93 analysis of spatial patterns of anthropogenic land use.

94 Furthermore, while human impact on the environment intensified with the introduction of agriculture, pre-
95 agricultural landscapes were already far from “natural” or “intact” (Ellis et al., 2021). Humans have a long
96 history of shaping their environments through niche construction activities (Nikulina et al., 2022), for example
97 through burning (Scherjon et al., 2015), and geographic range manipulations of plant and animal species
98 (Finsinger et al., 2006; Rowley-Conwy and Layton, 2011). Such alterations had a smaller immediate effect on
99 the environment compared to agriculture, especially industrial practices, but niche-constructing activities
100 spanned many thousands of years, dating back as far as the Last Interglacial (Roebroeks et al., 2021), with
101 numerous studies reporting cases of land-cover modifications over late Pleistocene and early Holocene
102 (Archibald et al., 2012; Bos and Urz, 2003; Doughty, 2013; McWethy et al., 2010; Pinter et al., 2011; Roberts
103 et al., 2021). Therefore, the cumulative effect of the prehistory-long legacy of non-agricultural human practices
104 on land-cover remains poorly understood.

105 Quantitative reconstructions of past vegetation cover indicate that changes of vegetation in Europe reach
106 maximum complexity in terms of the rate of change during the second half of the Holocene (from 8200-4200
107 BP to present day; hereafter, dates are expressed as calibrated calendar years before AD 1950 and referred to
108 as BP) (Marquer et al., 2014; Mottl et al., 2021). In Europe this period is characterized by the adoption of

109 agriculture and intensification of human-induced land-cover change (Stephens et al., 2019; Morrison et al.,
110 2021; Harrison et al., 2020; Goldewijk et al., 2017a; Kaplan et al., 2011; Gronenborn and Horejs, 2021) as well
111 as by a substantially changing climate (Arthur et al., 2022; Zhang et al., 2017). Moreover, analysis of the
112 European Pollen Database indicated that anthropogenic land-cover change in pollen records becomes
113 detectable from 6000 BP (Fyfe et al., 2015). Hence, in this study we focus on quantifying the anthropogenic
114 impact on European land-cover over the period of the second half of the Holocene (6200 BP – AD 2015).
115 Estimation of the magnitude of human-induced changes in land-cover is often performed through analysis of
116 palaeoecological data acquired from pollen-based reconstructions (Bartlein et al., 2011; Dallmeyer et al., 2019;
117 Marquer et al., 2017; Prentice et al., 1998; Strandberg et al., 2022). One of such reconstructions, the Regional
118 Estimates of VEgetation Abundance from Large Sites (REVEALS) model (Sugita, 2007a), was used to create
119 gridded pollen-based estimates of Holocene plant cover for NW-central Europe north of the Alps (five time
120 windows of the Holocene) (Trondman et al., 2015) and more recently for all of Europe through the Holocene
121 (11,700 BP to present) (Githumbi et al., 2022). The REVEALS reconstructions from Marquer et al., (2017) have
122 been used in the recent study of Dallmeyer et al. (2023), who applied an approach based on the comparison
123 between REVEALS-based reconstructions and land use forced vegetation model outputs for northern and
124 central Europe. Their study concluded that anthropogenic land use was the main driver of the decrease in
125 forest cover in Europe during mid- and late-Holocene (100 – 8000 BP). To further this analysis, we simulate
126 vegetation for the second half of the Holocene (6200 BP – AD 2015) and compare the results with an extended
127 version of the REVEALS-based reconstructions (Serge et al., 2023). Serge et al. (2023) used the same
128 protocol as described in Githumbi et al (2022) to produce the most spatially extensive and temporally
129 continuous pollen-based reconstructions of plant cover in Europe (at a spatial resolution of $1^\circ \times 1^\circ$ for 30° – 71°
130 N, 20° W– 47° E; spatial distribution is shown in Figure 2) over the Holocene at a temporal resolution of 500
131 years between 11,700 and 700 BP. For the most recent period, Serge et al. (2023) allocated smaller time
132 windows with a higher temporal resolution: 700–350 BP, 350–100 BP, and 100 BP–present (where the present
133 is the year of coring).

134 While indicating the significance of land use as a key factor in driving past land-cover change in Europe,
135 Dallmeyer et al. (2023) highlighted several challenges that arise when comparing pollen-based quantitative
136 vegetation reconstructions with outputs from vegetation models. In our current study, we address two of these

137 challenges: biases in simulated climate and distinction between anthropogenic and non-anthropogenic drivers
138 of land-cover change. To overcome these challenges, we propose a method that compares pollen-based
139 reconstructions with a theoretical state of vegetation cover - potential natural vegetation (PNV), which
140 represents climate-forced vegetation without human intervention or management (Hengl et al., 2018).

141 In this study, by analysing relationships between simulated PNV and pollen-based estimates of regional
142 vegetation abundance, we aim to (1) evaluate how far from natural conditions our REVEALS-based vegetation
143 is, by comparison with modelled potential natural vegetation, (2) quantify time-cumulative impact of human
144 modifications of European land-cover (accumulated impacts of human activity on natural ecosystems through
145 time) over the second half of the Holocene (6200 BP – AD 2015) including both agricultural and non-
146 agricultural human activities, and (3) assess the performance of the developed methodology through
147 comparison with existing ALCC scenarios KK10 and HYDE 3.2.

148 2. Methodology

149 2.1. Study design

150 In this study, we address the challenge of distinguishing between anthropogenic and non-anthropogenic
151 drivers of land-cover change. Pollen-based land-cover reconstructions allow the identification of phases of
152 vegetation compositional change comparable with periods of climate change, derived from independent
153 climate reconstructions to account for the importance of climate-driven vegetation change (Seddon et al.,
154 2014). However, the interaction of natural forces with anthropogenic influences induces complex processes
155 with profound effects on the environmental system (Kalis et al., 2003). It is thus not always easy to attribute
156 temporal changes in vegetation composition to a certain impact factor. The complex nature of interactions
157 between different impact factors often makes it difficult to distinguish between climatic and anthropogenic
158 origin of changes in vegetation patterns. Anthropogenic impact on vegetation composition is often derived from
159 pollen-based reconstructions using cultural indicators (e.g. Deza-Araujo et al., 2020; Behre, 1981). The
160 applicability of these indicators has been limited to regional studies due to regional variations in cultural
161 practices and vegetation dynamics. Recently, Deza-Araujo et al. (2022) suggested the use of agricultural land
162 use probability (LUP) index based on existing cultural indicators. This approach allows the use of the method
163 beyond the specific regions where the cultural indicators were developed. However, while promising, its

164 application to continental scales has not been explored. The relative importance of different impact factors for
165 various regions and time periods is, therefore, still a matter of debate (Marquer et al., 2017; Dallmeyer et al.,
166 2023). Moreover, quantifying the effect of early non-agricultural human practices (such as burning, wood
167 harvesting for different purposes, settlement activities, and geographic range manipulations of species) on
168 land-cover remains a challenging task, since these practices cannot be retrieved using cultural indicators that
169 target agricultural land use through the presence of representative taxa in pollen records, i.e. *Cerealia* type (t.)
170 (e.g. Githumbi et al., 2022; Gaillard, 2007). To tackle these challenges, analysis of pollen-based reconstructions
171 would benefit from comparison to a reference state that would represent vegetation over the studied time
172 period without anthropogenic changes of vegetation. Thus, in order to evaluate the extent of human-induced
173 land-cover change in Europe during the second half of the Holocene (6200 BP – AD 2015), we applied a
174 method that compares vegetation cover obtained through REVEALS-based reconstructions with an alternative
175 description of past vegetation cover – potential natural vegetation (PNV). The concept of PNV has been the
176 subject of past debate (e.g. Loidi et al., 2010; Jackson, 2013; Hengl et al., 2018; Somodi et al., 2012; Farris et
177 al., 2010). We consider that PNV describes a theoretical state of vegetation cover that would exist under the
178 assumption that the vegetation is in balance with environmental controls, such as climatic conditions and
179 disturbances, without any human intervention or management (Hengl et al., 2018). In a palaeoenvironmental
180 modelling context, PNV is often referred to an artificial construct simulated by a dynamic vegetation model
181 (DVM) without prescribed land use forcing, that represents climate-forced potential vegetation in the absence
182 of human-induced vegetation changes and other disturbances (e.g. wildfire, megafauna) (Trondman et al.,
183 2015). PNVs are routinely used in various modelling exercises, such as to evaluate vegetation naturalness
184 (Strona et al., 2016), analyse response of vegetation to climate change (Ren et al., 2021), or evaluate
185 reconstructions of past regional vegetation patterns (Cruz-Silva et al., 2022). A PNV distribution is often
186 simulated by vegetation models, which are based on modern empirical relationships between vegetation and
187 climate (Levvasseur et al., 2013). Taking advantage of the PNV concept as best available description of the
188 plausible vegetation of an area, we simulated PNV for the second half of the Holocene (6200 BP – AD 2015)
189 using the CARbon Assimilation In the Biosphere (CARAIB) dynamical vegetation model (Dury et al., 2011;
190 François et al., 2011; Laurent et al., 2008; Otto et al., 2002; Warnant et al., 1994), forced by downscaled bias-
191 corrected climate simulated by the iLOVECLIM model (Zapolska et al., 2023).

2.2. Design of the climate simulations

The climate simulations were performed with the iLOVECLIM model, version 1.1.5 (revision 1512). This model is a code fork of the original LOVECLIM 1.2 model (Goosse et al., 2010), revised by Roche (2013) and further expanded by Quiquet et al. (2018). In this study we used the online interactive downscaling method embedded in iLOVECLIM, first described by Quiquet et al. (2018). Our version of iLOVECLIM includes the following components: the atmospheric model, ECBilt (Opsteegh et al., 1998), the sea-ice ocean component, CLIO (Goosse and Fichefet, 1999), and the reduced-form dynamic global vegetation model, VECODE (Brovkin et al., 1997). We refer the reader to the reference articles for a complete description of the iLOVECLIM model (Roche, 2013) and downscaling method (Quiquet et al., 2018; Arthur et al., 2022).

Vegetation is an important component of climate dynamics, which impacts climate via physiological, biogeophysical and biogeochemical processes. It is, therefore, necessary to simulate vegetation cover to accurately simulate climate. This is why our climate simulations were performed with the VECODE reduced-form vegetation model (Brovkin et al., 1997) which computes plant and soil behaviours necessary to simulate the first order vegetation-climate feedback in climate models. Being a reduced-form DGVM, VECODE only computes 2 vegetation types: trees and grass (and bare ground as a dummy type). This is enough for the first order feedback to the atmospheric model, since it encompasses the three main classes affecting the albedo, the surface roughness and the link to the water cycle. However, it is far from being sufficient to reflect vegetation changes at the level of complexity needed for our main intercomparison with the REVEALS output, as described further in this study. This is why the resulting climatic evolution was then bias-corrected and used as an input to a much more complex vegetation model which has the necessary complexity to see the fine-scale structures we are concentrating on. The input was provided as climatologies (climatological means) of daily values for each time window (TW) (Supplementary table 1) without transient change in climate input (equilibrium simulations).

To summarise, the use of VECODE in the initial computation affected the large-scale climate providing the first-order response of dynamical vegetation coupled to climate at large scales, such as desertification (complete change from trees to grass or bare ground, and vice versa) or large shifts from forests to grassland. Fine-scale changes were then computed using the more complex (and more computationally intensive) CARAIB DGVM, so as to look into changes that are usually attributed to human impact on vegetation, such as

220 changes in vegetation composition which are far beyond the reach of the reduced-form VECODE model. The
221 coherency of the large-scale changes of the two vegetation models has been checked through the
222 intercomparison between the results of the two models, and the results showed that they are consistent in
223 patterns of large-scale vegetation response to climatic factors (not shown).

224 We applied iLOVECLIM to simulate the transient evolution of the climate during the Holocene. The
225 experiments were first initialised with a state derived from a 3,000 year long equilibrium simulation at 11,700
226 BP. Subsequently, we performed a full transient simulation from 11,700 BP up to present. Owing to the large
227 time scale response of the ocean and furthermore to the fact that the climate system is never in equilibrium
228 with forcing boundary conditions, we only considered the part 6,000 BP to present in our analysis, using the
229 section 11,700 BP to 6,000 BP as a further adaptation of climate to transient boundary conditions. For both
230 equilibrium and transient simulations, we used boundary conditions evolving as closely as possible to the state
231 of knowledge. Namely, we used astronomical parameters from Berger (1978), greenhouse gas levels (Schilt et
232 al., 2010; Raynaud et al., 2000), ice sheets from the GLAC-1D reconstruction (Tarasov et al., 2012; Tarasov
233 and Peltier, 2002) as well as evolving bathymetry and land-ocean mask coherent with those ice-sheet
234 geometries (with the same methodology as Bouttes et al., 2023). Between the year 6200 BP and the year 700
235 BP time windows (TWs) (Supplementary table 1) were assigned at 500 years temporal resolution, and the
236 lengths of the three most recent time windows were fixed to 350 (700 – 350 BP), 250 (350 – 100 BP), and 165
237 (AD 2015 - 1850).

238 The use of the model results for the intercomparison with pollen data in the context of the current study could
239 be considered indicative under assumption of minimal model biases. To correct biases of iLOVECLIM
240 modelled results, we applied the CDF-t bias correction technique (Vrac et al., 2012). CDF-t was previously
241 reported to yield significantly stronger agreement between the simulated results and pollen-based climate and
242 biome reconstructions, compared to modelled results without CDF-t application (Zapolska et al., 2023). A full
243 procedure of the bias correction methodology and its limitations can be found in Zapolska et al. (2023).

244 The observational reference dataset used for bias correction is the EWEMBI dataset (Earth2Observe, WATCH
245 Forcing Data (WFDEI), and ERA-Interim reanalysis data merged and bias-corrected for the InterSectoral
246 Impact Model Intercomparison Project) (Lange, 2016). The EWEMBI data covers 38 years from 1979 to 2016.
247 To match to the length of the observation dataset (which is required for the CDF-t methodology), we extracted

38 median years of 14 TWs (Supplementary table 1), consistent with the TWs of the REVEALS pollen-based land-cover reconstruction dataset for further analysis. Following the bias correction, each of 14 sets of climatic parameters was averaged to get daily mean climate characteristics of TWs.

The reliability of the described modelling workflow and the comparison of simulated climate and vegetation with available proxy data were evaluated in previous studies. Arthur et al. (2022) assessed the downscaled iLOVECLIM simulation for the Holocene before the application of CDF-t, while Zapolska et al. (2023) evaluated the downscaled iLOVECLIM and CARAIB performance for periods characterized by different climatic conditions with the CDF-t application.

2.3. Modelled potential natural vegetation

Potential natural vegetation was simulated using the CARbon Assimilation In the Biosphere (CARAIB) model (Otto et al., 2002; Laurent et al., 2008; Warnant et al., 1994; François et al., 2011; Dury et al., 2011) forced with 14 sets of climates simulated by the iLOVECLIM model (bias-corrected and averaged over TWs, as described above). The CARAIB model is composed of five modules describing respectively (1) the hydrological budget, (2) canopy photosynthesis and stomatal regulation, (3) carbon allocation and plant growth, (4) heterotrophic respiration and litter/soil carbon dynamics, and (5) plant competition and biogeography (François et al., 2011). In this study, we did not include the fire module in the simulations, and the fire regime was calibrated based on modern times. Water and carbon reservoirs in CARAIB are updated with a daily timestep, while photosynthesis and plant respiration are calculated every two hours to account for non-linear effects associated with the variation of photosynthetic/respiration fluxes over the day. The model simulates a given set of plant functional types (PFTs), which can coexist on the same grid cell. Trees are assumed to grow above herbs and shrubs (or bare ground), creating two vegetation levels with maximum coverage up to 1 at each level. Thus, the maximum vegetation fraction of a grid cell is 2, provided that both upper (trees) and lower (grass and shrubs) levels are fully vegetated. Vegetation cover output is updated every month for herbaceous PFTs and yearly for arboreal PFTs (François et al., 2011; Henrot et al., 2017). For a more detailed description of the CARAIB model we refer the reader to Otto *et al* (2002), Laurent *et al* (2008), Warnant *et al* (1994), François *et al* (2011), Dury *et al* (2011).

274 The input climatic fields used to run the CARAIB vegetation model were daily values of: (1) the mean near-
275 surface air temperature, (2) the daily amplitude of air temperature change, (3) precipitation, (4) air relative
276 humidity, (5) percentage of sunshine hours and (6) wind speed. In the current study, daily temperature
277 amplitudes and wind speed were taken from observations (Daily temperature amplitudes: Climatic Research
278 Unit (CRU) data, mean over 1901-2015; wind speed: EWEMBI dataset) and kept constant for all time periods.
279 Surface temperature, precipitation, relative humidity, and sunshine hours were derived from iLOVECLIM.
280 Biases in temperature, precipitation and relative humidity were corrected using the CDF-t approach (Vrac et
281 al., 2012). These sets of bias-corrected climate data were used to perform snapshot simulations with CARAIB
282 run until equilibrium (200 years), to obtain characteristic PNV patterns for the specified TWs.

284 2.4. The REVEALS Pollen-Based Land-cover Reconstructions

285 For comparison with the modelled PNV, we used a part of the last set of gridded pollen-based REVEALS plant-
286 cover estimates for 31 taxa at a spatial scale of $1^\circ \times 1^\circ$ across $30^\circ\text{--}71^\circ$ N, 20° W– 47° E (north-western, central
287 Europe, Mediterranean area, and part of the East until 47° E) for 14 contiguous time slices of 100-500 years
288 covering second half of the Holocene (Serge et al., 2023). Previous grid-based estimates (Githumbi et al.,
289 2022; Trondman et al., 2015) were designed for the purpose of conducting studies on the impact of land cover
290 on climate using climate models and DGVMs (Strandberg et al., 2022). The REVEALS dataset is the only
291 current land-cover reconstruction approach based on pollen data to quantify past regional cover of individual
292 plant taxa. It effectively accounts for intertaxonomic differences in pollen productivity and dispersal properties
293 as well as the size and type of sedimentary basins. It combined 1607 pollen records and benefited from earlier
294 efforts and projects (Landclim I and II) in collecting pollen dataset (Githumbi et al., 2022; Trondman et al.,
295 2015) obtained from databases and individual data contributors. There are many areas of Europe where
296 environments that preserve pollen (i.e. lakes, bogs, forest hollows) are sparse, therefore the geographic
297 distribution of pollen-based reconstruction is uneven.

298 REVEALS transforms pollen assemblages in large lakes to abundance of individual plant taxa in the
299 surrounding vegetation at a large spatial scale (ca. $100\text{ km} \times 100\text{ km}$; Hellman et al., 2008a, b) using a
300 mechanistic modelling approach that uses an empirical understanding of relative pollen production between

301 pollen morphological types, and pollen dispersal mechanisms. It was developed for pollen records from large
302 lakes (> 50-100 ha), but extensive simulation and empirical studies showed that multiple small-sized sites can
303 be used when large lakes are not available in a region, although it generally results in larger standard errors on
304 the estimates of plant cover (Sugita, 2007; Fyfe et al., 2013; Mazier et al., 2012; Trondman et al., 2015). As
305 previous studies (Mazier et al., 2012; Trondman et al., 2015; Githumbi et al., 2022), Serge et al., (2023) used a
306 1° resolution grid and applied REVEALS on all available pollen records in each grid cell to produce an estimate
307 of plant taxa abundance per grid cell through time. The estimates obtained for 31 individual taxa were later
308 summed to produce estimates of the area occupied by plant functional types according to Table 1. Estimating
309 the proportion of bare ground using pollen reconstructions is challenging due to the inherent limitations of the
310 data. Hence, in REVEALS data, the total cover of plant taxa within a grid cell is always 100%.

311 All gridded REVEALS reconstructions for Europe follow the same protocol and criteria as published in Mazier
312 et al. (2012) and Trondman et al. (2015), and lately by Githumbi et al. (2022). Gridded REVEALS estimates are
313 influenced by the quality of individual records used (pollen count size, taxonomic resolution, and chronological
314 uncertainty), basin size, and type of sites (lakes or bogs), the number of pollen records used in each grid cell,
315 and the reliability of the relative pollen productivities (RPPs) used (Githumbi et al., 2022; Trondman et al.,
316 2015; Serge et al., 2023). The precision of gridded REVEALS estimates is indicated by their standard errors.
317 Caution should be applied when using REVEALS estimates from unreliable grid cells, and when standard
318 errors of the gridded REVEALS estimates are equal or greater than REVEALS estimates (Serge et al., 2023).
319 Hence, the number of available REVEALS grid cells for analysis varies depending on the availability of reliable
320 pollen data for each TW. Across the 14 TWs studied here, the number of grid cells ranged from 456 to 363.
321 This range reflects variations in quantity and quality of the pollen data available for analysis during each time
322 window.

324 2.5. Classification of plant functional types

325 To reconstruct vegetation patterns and their changes throughout the Holocene we applied the concept of plant
326 functional types (PFTs). Plants were classified into PFTs based on their physical, phylogenetic and
327 phenological characteristics, as well as their bioclimatic and functional features. PFTs included in the CARAIB

328 model are described in François et al. (1998). In this study, each selected plant taxon was assigned to a
 329 specific unique PFT (Table 1) based on previously published classification used for model–data comparison in
 330 palaeovegetation studies (François et al., 2011; Henrot et al., 2017; Popova et al., 2013). Standard errors of
 331 the REVEALS dataset (Serge, 2023) were calculated for each PFT according to the delta method (Stuart and
 332 Ord, 1994).

CARAIB PFT	Short name	Plant taxa/pollen-morphological types (31 taxa)
Herbs (C3 herbs "humid", C3 herbs "dry", C4 herbs)	H	<i>Amaranthaceae /Chenopodiaceae, Artemisia, Cerealia t., Cyperaceae, Filipendula, Plantago lanceolata, Poaceae, Rumex acetosa t., Secale cereale</i>
Broadleaved evergreen boreal/temp cold shrubs	BEBTS	<i>Calluna vulgaris, Ericaceae</i>
Broadleaved evergreen temperate warm shrubs	BETWS	<i>Buxus sempervirens</i>
Needleleaved evergreen boreal/temp cold trees	NBTT	<i>Abies, Juniperus, Picea, Pinus</i>
Broadleaved evergreen meso-mediterranean trees	BEMMT	<i>Phillyrea, evergreen Quercus t.</i>
Broadleaved evergreen thermo-mediterranean trees	BETMT	<i>Pistacia</i>
Broadleaved summergreen boreal/temp cold trees	BSBTT	<i>Alnus, Betula, Corylus avellana, Salix</i>
Broadleaved summergreen temperate cool trees	BSTCT	<i>Carpinus betulus, Fagus, Fraxinus, deciduous Quercus t., Tilia, Ulmus</i>

Broadleaved summergreen temperate warm trees	BSTWT	<i>Castanea sativa</i> , <i>Carpinus orientalis</i> / <i>Ostrya</i> t.
---	-------	--

Table 1. Plant-functional types and corresponding plant taxa according to previously published classification used for model–data comparison in palaeovegetation studies (François et al., 2011; Henrot et al., 2017; Popova et al., 2013).

In CARAIB, plant growth in northern Europe is hindered by frigid climatic conditions of polar tundra, which prevents vegetation from populating the grid cells. Therefore, high latitudes in CARAIB are composed of bare ground with a few herbs (Supplementary Fig. 7). Pollen-based reconstructions, however, reflected presence of *Betula*, Ericaceae, Cyperaceae, *Pinus* and Poaceae in those areas across all studied TWs. A recent study of Sun et al. (2022) demonstrated the impact of the lack of representation of bare ground in REVEALS-based estimates. Hence, to eliminate some of the potential biases related to this issue, we chose to exclude high latitudes (70-71°N) from the intercomparison. With this we aimed to prevent the negative bias due to low agreement between the studied datasets over these zones, dictated by their technical characteristics. Furthermore, it is important for readers to exercise caution when interpreting regions with a high fraction of bare ground in the CARAIB model outputs (e.g., certain parts of the Iberian Peninsula) (Supplementary Fig. 7). The differences in the representation of bare ground across the studied datasets may increase the uncertainty of the analysis in these areas.

2.6. Comparison between REVEALS estimates and CARAIB simulations

Comparison of the CARAIB simulations with the REVEALS estimates required a transformation of the spatial and temporal resolution of the CARAIB model output. We aggregated the PNV simulated by CARAIB to the same grid resolution as the REVEALS estimates (1°x1° grid cells) and extracted only those grid cells where the pollen data were available (ranging from 456 to 363 grid cells for the analyzed TWs). CARAIB vegetation is represented by two vertical layers that were adjusted to match a resolution of 1°, used by the REVEALS method.

Then, relationship between REVEALS and CARAIB was analysed by computing a weighted matching ratio between PFT fractions of both models, using the following formulas:

$$MR_{PFT} = \text{frac}_{PFT, \text{reveals}} \div \text{frac}_{PFT, \text{caraib}} \times 100 \text{ ,}$$

and

$$WMR = \sum_{PFT=1}^{Nb.PFT} \text{frac}_{PFT, \text{reveals}} \times MR_{PFT} \text{ ,}$$

where Nb.PFT – maximum number of PFTs, $\text{frac}_{PFT, \text{reveals}}$ – fraction of a PFT in REVEALS dataset, $\text{frac}_{PFT, \text{caraib}}$ – fraction of corresponding PFT in CARAIB dataset, MR_{PFT} – matching ratio per PFT, WMR – weighted matching ratio of REVEALS and CARAIB.

Similarity between CARAIB and REVEALS estimates per PFT was expressed in matching ratio (MR) values. Considering that the two datasets are independent and of a different nature, the use of absolute values of MRs for the intercomparison could have been challenging due to limitations and biases of the methodology. Such biases remain in all TWs (assuming their stationarity), but MRs may not be constant through time. In this study it is assumed that this variation occurs due to human impact, which is the factor that is not stationary in time throughout our study period. Therefore, we focused on temporal changes within PFTs rather than absolute differences between the datasets to minimize the impact of such biases on our results. To this end, we have chosen to analyze the relative change in the MR values between each TW and the TW calculated in the most recent period (TW1).

WMR was calculated to ensure that more weights are given to the PFTs that are more abundant within a grid cell. Under an assumption that WMR represents percentage of vegetation unaltered by anthropogenic activity, by reversing it we calculate a human pressure index (HPI):

$$HPI = (100 - WMR) \div 100.$$

Then, a mean HPI over each 1°-wide latitudinal zone was calculated for each TW.

Translating the discrepancies between the two studied datasets into the HPI was made under the assumption that changes in relationship between the two datasets at the second half of the Holocene are mainly caused by anthropogenic activity. This assumption is supported by a growing body of evidence, including palaeoenvironmental reconstructions, that suggests a significant and widespread impact of human activities on European land-cover during this period (Roberts et al., 2019, 2018; Ruddiman and Ellis, 2009; Nielsen et al.,

2012; Kaplan et al., 2009; Ellis et al., 2013; Strandberg et al., 2022). While megafauna presence is also not simulated by PNV models, the extinction of many megafaunal species during the late Pleistocene and the Holocene in Europe (Mann et al., 2019; Sandom et al., 2014; Stewart et al., 2021; Koch and Barnosky, 2006) decreases their potential role in large-scale changes in vegetation patterns over the second half of the Holocene. Taken together, these lines of evidence support our assumption that anthropogenic activity is the main driver of changes in the relationship between the datasets during the second half of the Holocene.

2.7. Correlation with ALCC scenarios

In order to compare our results with existing literature on anthropogenic impact on European land-cover, we used two most commonly used in landscape research ALCC scenarios, KK10 and HYDE 3.2. ALCCs offer the advantage over other datasets as they provide datasets that are continuous in space and time, whilst other approaches (for example, demographic proxies such as archaeological dates (e.g. Shennan et al., 2013), or human impact indicators from pollen data) have discontinuous coverage, and are not necessarily linearly related to land cover changes (Hiscock and Attenbrow, 2016). KK10 and HYDE 3.2 differ in the way they estimate and represent land-cover change. KK10 consists of data expressed in a form of a deforestation index at annual resolution, which, in this study, was averaged over the years within each of the REVEALS time windows (Supplementary Table 1). HYDE 3.2 estimates are presented in a form of simulated land use. In this study, to represent anthropogenic land use for agricultural purposes we analysed HYDE 3.2 data on croplands and grazing. HYDE 3.2 data is irregularly spaced in time over the Holocene: from 100 years temporal resolution in the Late Holocene to 1000 years in the early and Mid-Holocene. We used linear interpolation to obtain the data for the studied time windows. We also performed transformations of spatial resolution of both ALCC scenarios by aggregating the grid cells to the 1°x1° REVEALS grid, and extracted data only for the grid cells that have available data in REVEALS.

For comparison between HPI and KK10 and HYDE, we assumed that extracted land use from the ALCC scenarios should be roughly equivalent to human impact on land-cover. We then analysed correlation between these three datasets to investigate if they represent human-induced land-cover changes in a similar manner. Additionally, we evaluated the relationship between HPI values and HYDE 3.2 population density estimates to

409 understand if presence of humans spatially correlates with changes in HPI. HYDE 3.2 population density is
410 primarily based on demographers' estimates for the last 3000 years (McEvedy and Jones, 1978), with earlier
411 population sizes being estimated using back extrapolation (Goldewijk et al., 2010).

412

413

414

415

3. Results

416

417

We have analysed palaeovegetation data expressed in fractions of PFTs for 14 TWs throughout the second half of the Holocene (6200 BP – AD 2015) from CARAIB simulations (representing PNV) and REVEALS

418

419

estimates (representing pollen-based regional vegetation abundance). The definitions of TWs are summarised in Supplementary Table 1.

420

421

The analysis of the relationship between simulated PNV and pollen-based regional estimates of vegetation

422

abundance is based on the evolution of discrepancies in the two datasets and expressed as relative change in

423

the MR values between each TW and the TW calculated in the most recent period (TW1) (Fig.1). Throughout

424

the studied time period, we observe decreases in MR of herbs (H), broadleaved summergreen

425

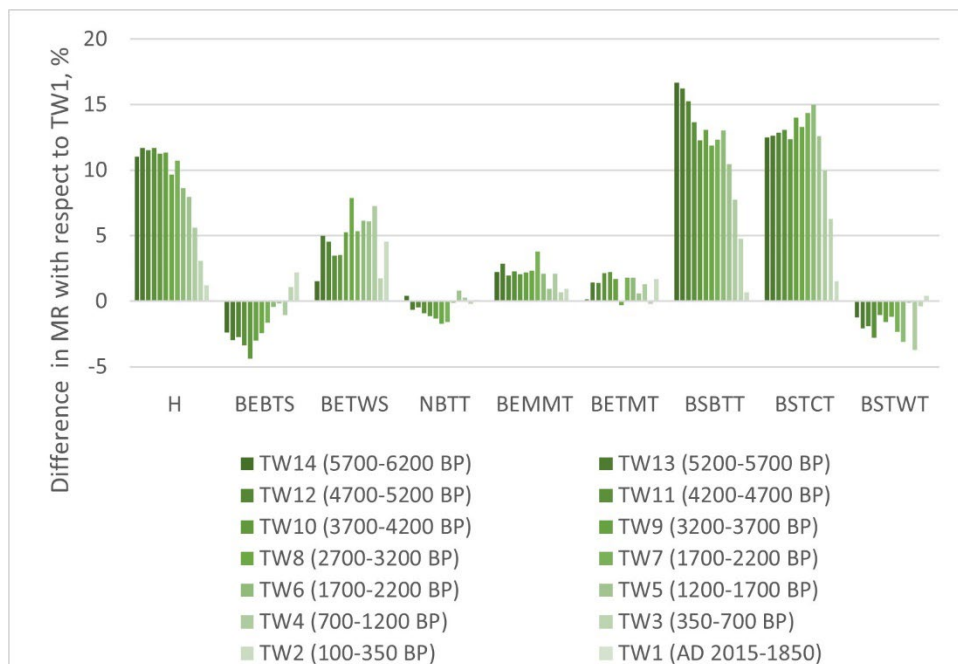
boreal/temperate cold trees (BSBTT) and broadleaved summergreen temperate cool trees (BSTCT). MR of

426

broadleaved evergreen boreal/temperate cold shrubs (BEBTS) increases, and MR of broadleaved evergreen

427

temperate warm shrubs follows a non-linear trend.



428

429

Figure 1. Temporal evolution of agreement per PFT between the CARAIB simulations and the

430

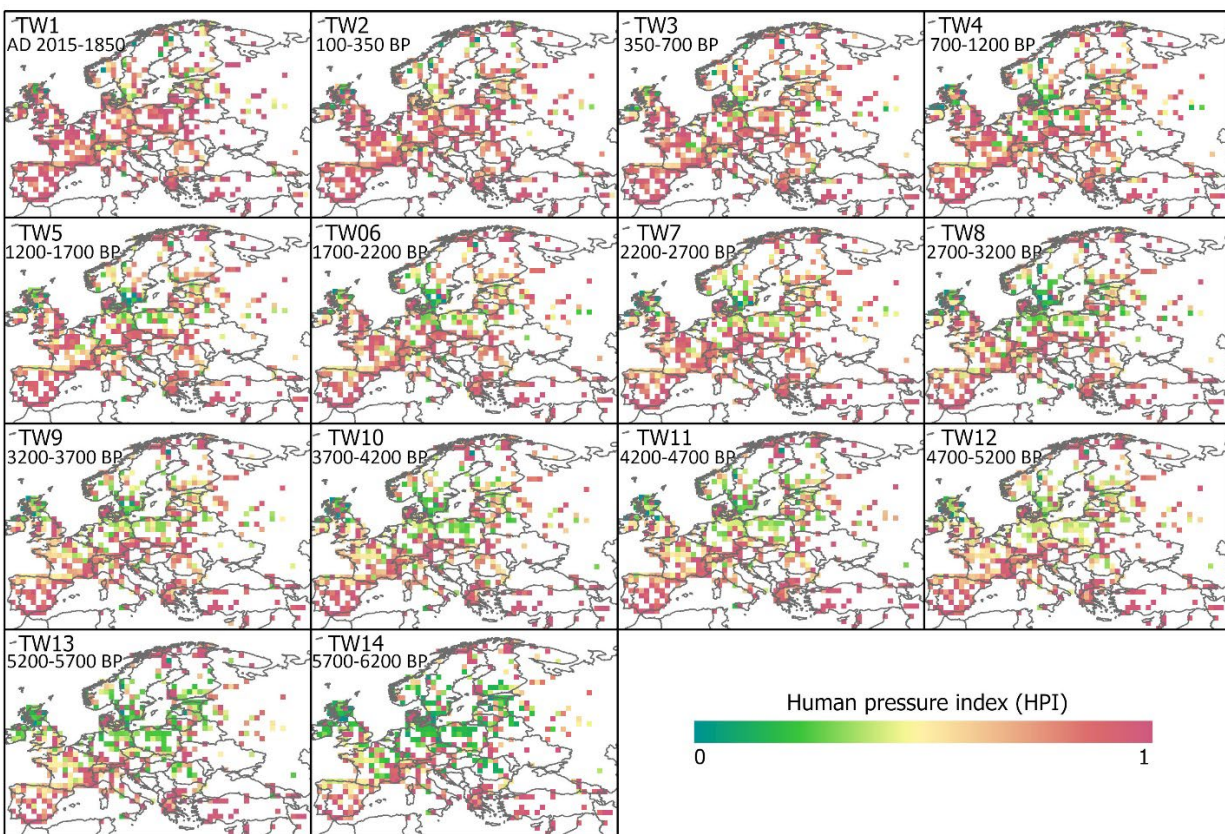
REVEALS estimates expressed as difference in matching ratio (MR) from MR at TW1 (present - 100

431

BP).

432 Figure 1 shows that different PFTs had different levels of dissimilarities and evolved differently through time.
433 Therefore, to analyse anthropogenic impact on vegetation dynamics that would account for all the changes
434 within PFTs we introduce a human pressure index (HPI). HPI is calculated based on matching ratios of
435 individual PFTs for each grid cell, and the weight of the variables is determined by the abundance of each PFT
436 in the REVEALS estimates.

437



438

439 Figure 2. Human pressure index per grid cell in Europe from TW14 (5700 - 6200 BP) to TW1 (present - 100
440 BP). 1-highest human pressure; and 0-lowest human pressure value.

441 We observe high HPI values at 5700-6200 BP (TW14) across the Mediterranean region and eastern Europe
442 (Fig. 2). Throughout the Holocene HPI values become progressively higher in central, western and northern
443 Europe, with the majority of the grid cells having extremely high HPI values at modern time (TW1) across the
444 continent. During the whole studied period high HPI is observed in northern Europe (Scandinavia), which is an
445 artefact of intrinsic biases of two datasets compared (Section 4.4). Hence, the high latitudinal zones (70-71°N)
446 are not included in the subsequent analyses.

447 In Figure 3, we subdivide our study area into latitudinal zones of 1 degree, corresponding to the size of grid
448 cells used for our analysis. This division allows us to display latitudinal trends of HPI changes through the
449 second half of the Holocene in Europe. We chose to present the dynamic per latitudinal zone based on the
450 historical context of our study period in Europe, which corresponds to the transition and establishment of
451 agriculture (Stephens et al., 2019; Morrison et al., 2021; Harrison et al., 2020; Goldewijk et al., 2017a; Kaplan
452 et al., 2011; Gronenborn and Horejs, 2021). Archaeological sources (e.g. Gronenborn and Horejs, 2021;
453 Stephens et al., 2019) provide evidence that this agricultural transition followed a south-to-north trend, with
454 agriculture being established first in the Mediterranean region, and gradually expanding northward. While we
455 acknowledge that this is an oversimplified description of the complex dynamics of the processes involved, by
456 presenting the data in this manner, we visualize the general temporal trend of HPI increase, potentially largely
457 affected by the agricultural expansion.

458 Vegetation of mid-latitudes resulted to be relatively preserved at earlier times. Contrastingly, Southern latitudes
459 (37.5 °N to 41.5 °N) have relatively high HPI throughout the studied period. 42.5 °N to 54.5 °N are the areas
460 where the changes are the largest within the studied timeframe, demonstrating a northward direction of HPI
461 increase in time through the second half of the Holocene.

462 Although there are limitations to the methodology used in our study that affect the robustness of our results in
463 northern latitudes, we observe a clear and gradual increase in HPI over time at latitudes south of 54.5°N (Fig.
464 3), which covers a large part of continental Europe. This enables us to track the long-term dynamics of human
465 activity on land-cover across both time and space for a significant portion of the continent, which is where the
466 majority of vegetation changes have occurred.

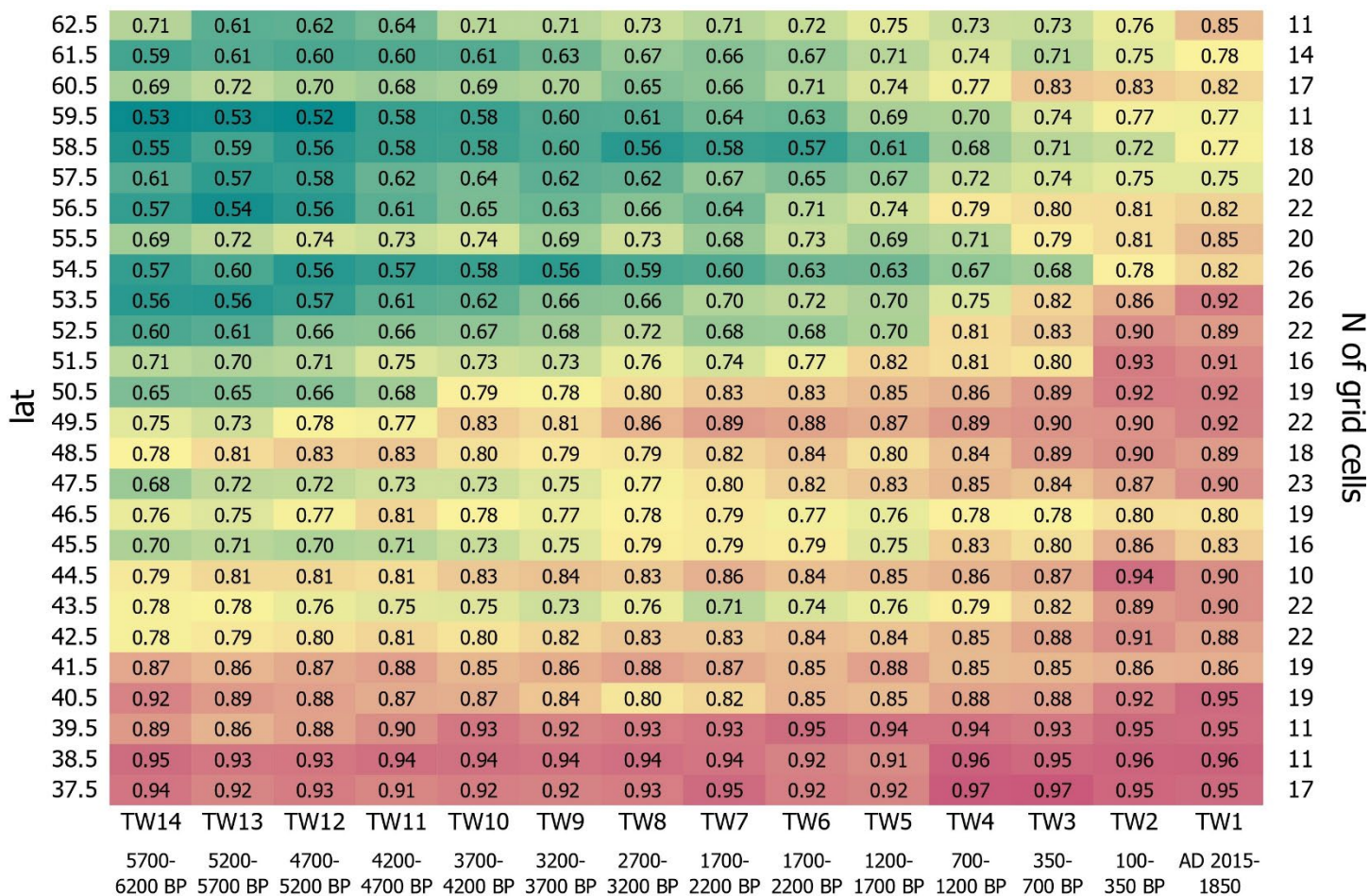


Figure 3. Human pressure index (HPI) over latitudinal zones in Europe from TW14 (5700 - 6200 BP) to TW1 (present - 100 BP). 1-highest human pressure; and 0-lowest human pressure value. Zones with less than 10 grid cells are not shown.

To determine statistical significance of our results, and their evolution in comparison to present day, we calculate the percentage of grid cells with HPI values significantly different from the modern time TW1 at the 0.05 level (paired Student's t-tests). Figure 4 illustrates that the percentage of grid cells with values that indicate significantly lower human pressure compared to modern values (N-S) decreases as we move from early time to modern time, indicating that roughly 60% of grid cells had significantly lower HPI (are significantly less impacted by human activity) at 5700-6200 BP, compared to modern values.

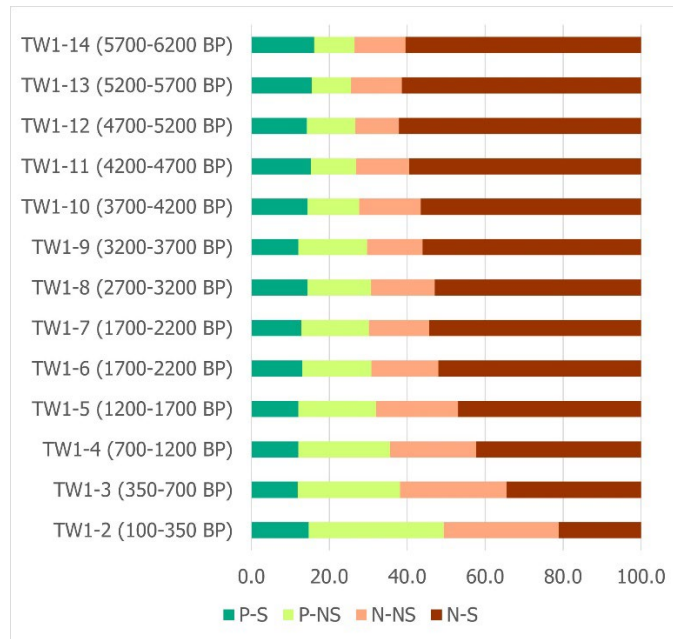


Figure 4. Percentage of grid cells with indicated difference in HPI between the TW1 (AD 2015-1850) and each consequent TW. P: positive slope (the most recent time window has lower human pressure index); N: negative slope (the most recent time window has higher human pressure index); S: significant; NS: non-significant at the 0.05 level (paired Student's t-tests). For example, for the difference between TW14 and TW1, the dark brown part of the bar shows that 60% had a statistically significant negative slope, indicating that TW1 had a significantly higher HPI value than TW14. For the maps of the differences in HPI please refer to the Supplementary Fig. 1, 2.

Overall, across Europe our results indicate a gradual increase of HPI throughout the second half of the Holocene (Fig.5), which escalated after TW5 (1200-1700 BP). Moreover, at the beginning of our simulation (TW14) we observe an average HPI of 0.72, which suggests that vegetation cover in Europe at 5700-6200 BP corresponded to modelled potential natural state of vegetation only for nearly 30%.

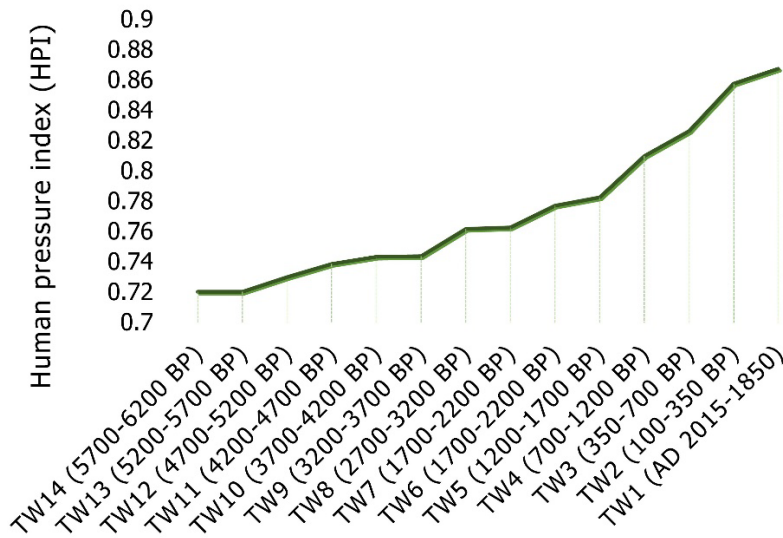


Figure 5. Human pressure index (HPI) in Europe from TW14 (5700 - 6200 BP) to TW1 (present - 100 BP).

Re-analysis of the KK10 and HYDE 3.2 estimates at REVEALS spatio-temporal resolution reveals that HYDE 3.2 cropland and grazing area increase (Fig.6, left), and KK10 deforestation for agriculture rise (Fig.6, right) follow similar patterns to HPI increase (Figure 5). However, the initial HPI values at TW14 are significantly higher than anthropogenic land use change compared to the rates of spread of agricultural practices (Supplementary Fig. 3,4).

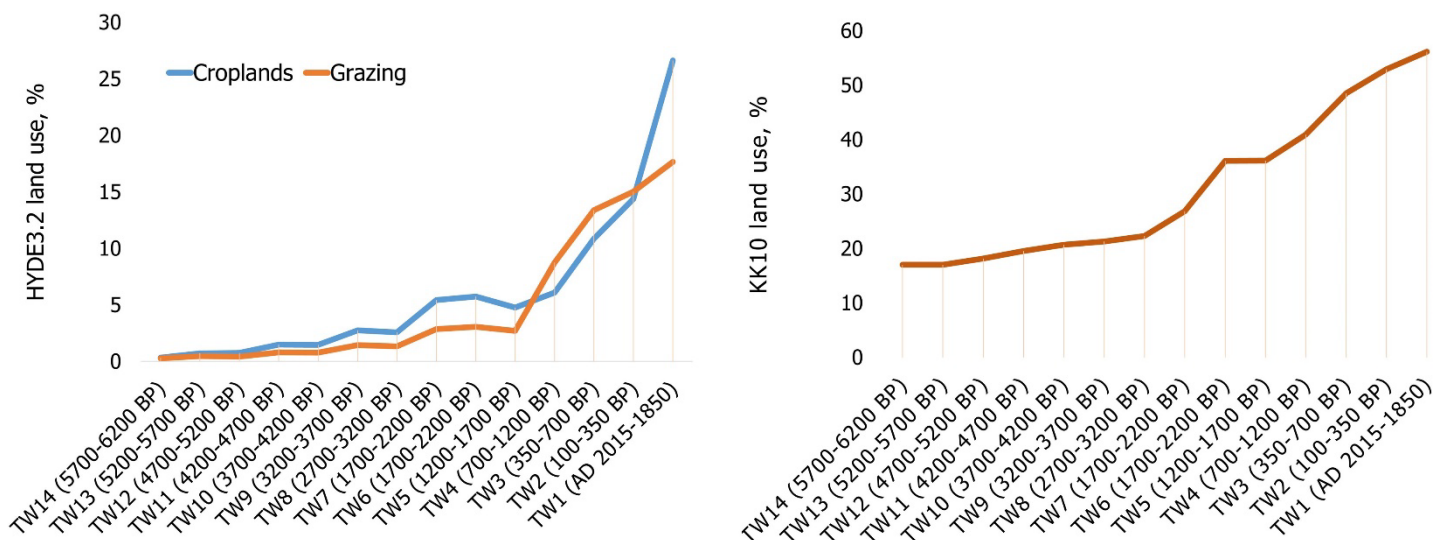
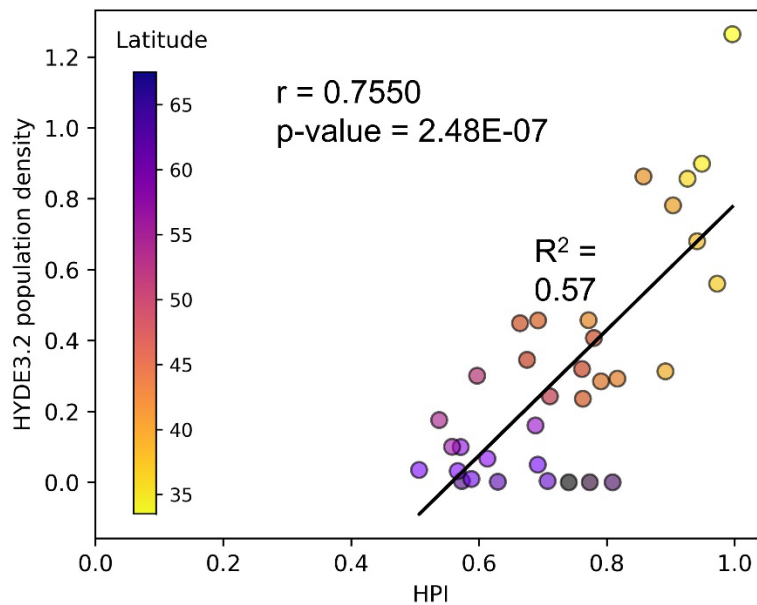


Figure 6. HYDE 3.2 simulated land use, expressed as fraction of croplands and grazing per grid cell (left panel), and KK10 simulated land use, expressed as deforestation index (right panel).

500 To further investigate the relationship between HPI and agriculture, we analyse the onset of agriculture in
501 REVEALS vegetation reconstructions, marked by first appearance of *Cerealia t.* and *Secale cereale* pollen in
502 the dataset. We assume that the agricultural onset is represented as a year of the earliest (within the time
503 bounds of our study) appearance of the aforementioned agricultural taxa in REVEALS at each grid cell
504 (Supplementary Fig. 6). However, the identification of the onset of agriculture based on agricultural PFT in
505 REVEALS is constrained by the limitations of this approach, described by Trondman et al. (2015). We,
506 therefore, do not identify patterns similar to the onset of agriculture in Europe described by the existing
507 anthropogenic land-cover change (ALCC) scenarios.

508 Additionally, we explore the correlation between HPI and ALCC simulated agricultural practices. Although we
509 observe a weak correlation between the two variables (Supplementary Fig. 3-4), the HPI index at 5700-6200
510 BP is significantly correlated with HYDE 3.2 population density estimates (Fig.7), thus reflecting human
511 presence in landscapes.



512

513 Figure 7. Correlation between human pressure index (HPI) versus HYDE 3.2 population density
514 estimates over latitudinal zones in Europe for TW14 (5700-6200 BP).

515

516

4. Discussion

Analysing land-cover change in Europe using REVEALS estimates and independent climatic and land use data, Marquer et al. (2017) suggested that climate is a major driver of vegetation change during the Holocene as a whole and at the sub-continental scale, stating that the land use impact increase gradually after 7000 BP while identifying four critical phases of land use effects on vegetation. Our methodology compared REVEALS estimates with simulated climate-only-driven potential natural vegetation (PNV) over the studied period to discount from the analysis changes in vegetation that were predominantly caused by changing climate. Previous studies suggest that climate change and anthropogenic activity are assumed to be the main driving factors of land-cover change in Europe over the second half of the Holocene (Marquer et al., 2017; Strandberg et al., 2022; O'Dwyer et al., 2021; Kuosmanen et al., 2018; Poska et al., 2022; Roberts et al., 2019, 2018). Thus, the difference between the two types of vegetation was introduced as a human pressure index (HPI). This index represents how different reconstructed vegetation is from a natural state, and thus includes both direct (*i.e.* deforestation and plant cultivation) and indirect (through biogeochemical feedbacks) anthropogenic changes in vegetation composition. These changes reflect continuous and prolonged human impact on European land-cover through various practices, which accumulated their consequence over time, building up a cumulative human pressure.

4.1. Fire regime

In this study, CARAIB simulations did not include the fire module, and thus, the potential impact of wildfires could contribute to dissimilarities between PNV and vegetation reconstructions. The studied period in Europe is covering a transition from hunter-gatherer to agricultural societies (Stephens et al., 2019; Gronenborn and Horejs, 2021). Human induced biomass burning was previously linked to both agricultural (*i.e.* slash-and-burn) (Vanni re et al., 2016) and non-agricultural practices (*i.e.* initiating selectively support food growth, tool in social interactions, or keeping away predators) (Scherjon et al., 2015). Thus, fires throughout the studied period were expected to have predominantly anthropogenic origin, which reflects human pressure on land-cover, and thus contributes to increase in HPI. Previously, sedimentary charcoal composites analysis revealed that humans have significantly influenced fire activity throughout the Holocene in Europe (Dietze et al., 2018; Connor et al., 2019; Vanni re et al., 2016; Carracedo et al., 2018), and outlined that human impact on fire regime could be both direct (*via* its use as a land management tool) and indirect (*via* affecting biogeochemical

545 cycles and increase landscape flammability) (Dietze et al., 2018; Connor et al., 2019). Thus, the wildfire regime
546 of the studied period was also altered by human activities, which brings additional challenges to making a clear
547 distinction between “natural” and “anthropogenic” fires (e.g. Vanniére et al., 2015; Power et al., 2008). Due to
548 not having available methods to separate natural from human-induced fires, and assuming minor role of
549 natural fires in the analysis compared to anthropogenic impact on land-cover change, wildfires were not
550 explicitly included in our analysis.

551 4.2. Insight from REVEALS dataset analysis - comparison with previous studies

552 Previously, land-cover naturalness and anthropogenic impact on vegetation were assessed through analysing
553 changes in forested areas (Strona et al., 2016; Kaplan et al., 2017; Pirzamanbein and Lindström, 2022;
554 Woodbridge et al., 2018) and via cultural indicator-types in pollen sequences (Deza-Araujo et al., 2022, 2020;
555 Behre, 1981; Mercuri et al., 2013; Gaillard, 2013; Mazier et al., 2006, 2009). Apart from known cultivars, many
556 cultural indicator pollen types are components of natural vegetation, characteristic of open conditions, natural
557 grazing dynamics or disturbed soils, particularly in southern Europe (Fyfe et al., 2019; Roberts et al., 2019) and
558 thus require careful interpretation. Within the framework of the LANDCLIM project (Gaillard et al., 2010)
559 anthropogenic land-cover changes were commonly expressed as vegetation openness indicated in the
560 REVEALS model results (Trondman et al., 2015).

561 Recently, REVEALS estimates were compared with DVM-simulated vegetation with a goal of assessing land-
562 cover change in Europe and analysing underlying processes behind the observed changes (Dallmeyer et al.,
563 2023). Similar to our study, Dallmeyer et al. (2023) attributed varying discrepancy over time between the two
564 datasets to human activity. Here we applied a more complex approach that takes into account vegetation
565 composition in the form of fractions of plant functional types (PFTs) and their evolution through time, and used
566 more spatially explicit REVEALS estimates. We identified that in addition to vegetation openness (expressed
567 as fraction of herbaceous cover), anthropogenic changes affected distribution of other PFTs, such as
568 broadleaved summergreen boreal/temperate cold trees (BSBTT), broadleaved summergreen temperate cool
569 trees (BSTCT), broadleaved evergreen boreal/temperate cold shrubs (BEBTS), and broadleaved evergreen
570 temperate warm shrubs (BETWS) (Fig.1). Lechterbeck et al. (2014) also found that early agriculture resulted in
571 compositional changes in forests in southern Germany, rather than increased openness.

572 Analysing the REVEALS dataset, Marquer et al. (2017) indicated a decrease of broadleaved forest and an
573 expansion of coniferous woodland during the Mid-Holocene. Our findings support the hypothesis about the
574 anthropogenic nature of changes in broadleaved summergreen PFTs (BSBTT and BSTCT) (Fig. 1). However,
575 contrastingly to Marquer et al. (2017), we observed no significant variation in MR of needleleaved evergreen
576 plant group (NBTT), which suggests that the coniferous woodland expansion reported by Marquer et al. (2017)
577 is likely driven by climatic factors. In addition to changes in vegetation openness and herbs (such as
578 *Filipendula*, *Artemisia*, *Plantago* and *Rumex acetosa* t.) (Gaillard, 2007), anthropogenic activity in REVEALS
579 estimates were previously attributed to changes in agricultural taxa (*Cerealia* t. and *Secale cereale*) (Trondman
580 et al., 2015). Our results supported the hypothesis about anthropogenic nature of changes in openness,
581 represented by the fraction of herbs. However, we observed the absence of statistically significant difference in
582 HPI values between grid cells with and without the presence of agricultural taxa in REVEALS (Supplementary
583 Fig. 5). The observed results may be attributed to the representation of agricultural land in REVEALS
584 reconstructions. For example, the classification does not include other cultivated plants, such as *Fagopyrum*
585 (buckwheat), *Linum usitatissimum* (common flax) and *Juglans regia* (walnut) (Trondman et al., 2015). This
586 suggests that the HPI reflects human pressure on vegetation in a more broad sense than just *Cerealia* t. and
587 *Secale cereale* crop cultivation.

588 4.3. Consistency of our findings with ALCC scenarios

589 Contrastingly, the evolution of HPI patterns through the studied period generally coincide in time and location
590 with previously simulated by ALCC human induced vegetation changes. Anthropogenic impact on land-cover
591 was previously reported to shift north throughout the second half of the Holocene (Goldewijk et al., 2017;
592 Kaplan and Krumhardt, 2011; Stephens et al., 2019), which is reflected in HPI values, which rise following
593 similar trajectory (Fig. 3). Moreover, at 6000 BP our results present a general agreement in patterns of HPI
594 with the KK10 ALCC scenario (Kaplan and Krumhardt, 2011). Both indicate anthropogenic land-cover
595 modifications across Mediterranean Europe and partial modifications in central and northern Europe (Figure 2,
596 Supplementary Fig. 1). The areas of high human pressure index coincide with the spread of agriculture,
597 indicated in the HYDE 3.2 ALCC (Goldewijk et al., 2017a). However, HPI indicated higher anthropogenic land-
598 cover change at 6000 BP than KK10 and HYDE 3.2 in eastern Europe, which is not reflected in either of the
599 two ALCC. It should be noted that both ALCC scenarios are derived from GIS models that are primarily based

600 on population estimates and geographic information (Marquer et al., 2017; Kaplan et al., 2009; Goldewijk et al.,
601 2017a). Therefore, they are constrained by various methodology limitations and do not always agree with
602 archaeological records. For example, findings of KK10 and HYDE 3.2 scenarios for eastern Europe differ from
603 conclusions of the ArchaeoGLOBE project, an empirical global assessment initiative of land use based on
604 archaeological knowledge (Stephens et al., 2019). ArchaeoGLOBE results suggested that the onset of
605 intensive (in the case of HYDE 3.2) and widespread agriculture (in the case of both KK10 and HYDE 3.2) in the
606 region was significantly underestimated (for up to 7500 years) in both ALCC scenarios. According to
607 ArchaeoGLOBE estimates, common levels of intensive agriculture onset in the region were present at 6000 BP
608 (Stephens et al., 2019), which supported our results, indicating relatively high HPI values over the region in the
609 Mid-Holocene (Fig. 2).

610 In our findings, we observed nearly 60% of grid cells to have a significant increase in HPI values at TW1 (AD
611 1850 – 2005), compared to TW14 (5700-6200 BP) (Fig. 4). Since this period is characterised by the onset and
612 spread of agriculture over the study region (Stephens et al., 2019; Kaplan and Krumhardt, 2011; Goldewijk et
613 al., 2017a), we assumed this value to be largely attributed to agricultural activity. Reported increase in HPI
614 agrees with the ALCC estimates and FAO land use statistics (FAO, 2022), which reports that 52.3% of the
615 area of European Union was 1961 classified as agricultural. Similarly, the ALCC scenarios suggest that for the
616 study area at TW1 (modern time) nearly 56% of land-cover was transformed by anthropogenic activity
617 accordingly to KK10, and HYDE 3.2 estimates suggested nearly 45% of land-cover to be impacted by
618 agriculture (18% grazing and 27% cropland) (Fig.6). ALCC estimates agree with the FAO land use statistics
619 (FAO, 2022), since they are partially based on FAO statistics (in case of HYDE 3.2). In this study we analysed
620 data for continental Europe, contrastingly to FAO land use statistics, which is constrained by the EU borders.
621 Additionally, the REVEALS dataset is not spatially continuous. Thus, the values in Figure 6 are not directly
622 comparable to FAO statistics. However, the ALCC land use indices at TW1 have similar levels of magnitude to
623 extent of agricultural land reported by FAO, confirming that both KK10 and HYDE 3.2 mainly represent land-
624 cover change for agricultural purposes, and indicating that the HPI detected land-cover change for agricultural
625 purposes in a similar manner to analysed ALCC scenarios.

626 We note that agriculture appeared in Europe as early as ca. 8000 – 9000 BP (Stephens et al., 2019;
627 Gronenborn and Horejs, 2021), and by the earliest TW covered in this study (5700-6200 BP), it had become

widespread in some European regions (Stephens et al., 2019). Consequently, high HPI values at that period are to a degree attributed to early agricultural practices, particularly in the Mediterranean region and Southern Europe (Fig. 2,3). However, HPI shows a significantly larger anthropogenic land-cover change at TW14 (5700-6200 BP) than the two considered ALCCs (Fig. 5,6 Supplementary Fig. 3,4). Considering the fact that land-cover changes in KK10 and HYDE 3.2 reflect the establishment of the first agricultural societies (Goldewijk et al., 2017b; Kaplan et al., 2009), and show 17% and 0% of agriculture-driven landscape changes at TW14 correspondingly (Fig. 6), we suggest that high HPI values at TW14 (Fig. 3,5) are partially attributed to pre-agricultural anthropogenic land-cover modifications that accumulated throughout the history of human-environment interactions in Europe and led to high levels of vegetation divergence from potential natural state. These findings emphasize the importance of accounting for early anthropogenic landscape impact, reported in previous studies (Archibald et al., 2012; Bos and Urz, 2003; Doughty, 2013; McWethy et al., 2010; Pinter et al., 2011; Roberts et al., 2021; Ellis et al., 2021; Nikulina et al., 2022).

4.4. Methodological limitations

It should be noted that the overestimation in HPI could be partially attributed to methodology limitations. Such limitations were caused by data availability in the REVEALS dataset, as well as by unequal reliability of the REVEALS grid cells (Serge et al., 2023). The intercomparison between reconstructed and modelled vegetation was also previously reported to be challenging (Dallmeyer et al., 2023). In addition, to correct biases of the used climate model we used the CDF-t approach (Vrac, 2018; Zapolska et al., 2023), but no bias correction was performed for the vegetation model (CARAIB). For the intercomparison PNV data was resampled and reclassified to be compatible with the REVEALS dataset, which in turn led to simplifications and resampling biases. For example, as in this work we assigned each taxon to a unique PFT category, the taxon Ericaceae was only included in broadleaved evergreen boreal/temperate cold shrubs (BEBTS) PFT (Table 1). However the Ericaceae family includes species that live both in the north and at high elevations (herbs and low shrubs, i.e. *Vaccinium*, *Arctostaphylos uva-ursi*), and in the South (trees, i.e. *Arbutus unedo*, *Erica arborea*) (Serge et al., 2023).

We hypothesise that the descending temporal trend and high HPI values in northern latitudes were mainly caused by the aforementioned methodology biases, such as PFT classification limitations and differences in representation of bare ground in studied datasets. Moreover, the trees at high latitudes might be confined in

656 small topographic depressions that induce a local micro-climate that we cannot reproduce at our spatial scale.
657 However, the rising HPI values through the studied period in most of continental Europe (south of 54.5°N) were
658 mainly associated with human activity, which was previously reported to shift north throughout the second half
659 of the Holocene (Goldewijk et al., 2017a; Kaplan and Krumhardt, 2011; Stephens et al., 2019).

660 4.5. Quantifying uncertainties

661 It should be noted that the absolute HPI values (Fig. 2, 3, 5) should be treated with caution, as they are
662 affected by various methodology biases discussed in this study. To our knowledge, there is no approach to
663 quantify given uncertainties. However, the study of Zapolska et. al (2023) estimated methodological
664 uncertainties of the used approach by comparing PNV simulations from bias-corrected CARAIB and
665 statistically modelled PNV distribution of Levavasseur et al., (2012), based on BIOME6000 pollen
666 reconstructions. Their findings indicate that methodological biases can constitute up to nearly 50% when
667 analysing matching ratios between PNV datasets of a different origin, which would place a lower boundary on
668 the HPI absolute value at 6000 BP (Fig.5) at about 30%, but likely more if median taken. To eliminate the
669 impact of these biases on our conclusions, we emphasise the importance of changes from one TW to another,
670 rather than absolute differences between the datasets, as the impact of methodology biases remains constant
671 in all TWs (assuming their stationarity). Hence, our conclusions are largely based on the analysis of temporal
672 changes in HPI values and trends that appear in these changes.

673 To verify our findings, further studies aimed at evaluation of human pressure on land-cover could compare the
674 results using several vegetation models (*i.e.* Dallmeyer et al., 2023), undertake a detailed intercomparison with
675 established and emerging pollen-indicator type approaches (e.g. Deza-Aruajo et al., 2022), draw on more
676 extensive compilations of pollen records, as well as investigate potential impact of bare ground in pollen-based
677 reconstructions (e.g. through the application of the Modern Analogue Technique demonstrated by Sun et al.,
678 2022). In addition, incorporating ALCC estimates in the workflow and introducing plant consumption by
679 megafauna would allow further analysis of underlying processes behind detected land-cover changes.

681 4.6. More than agriculture – pre-agricultural practices and land-cover naturalness

682 Despite the limitations of our study, the significant relationship between the HPI and HYDE 3.2 population
683 density (Fig.7) supported the suggestion that relatively high HPI values in the Mid-Holocene were mainly
684 attributed to human vegetation cover modifications by the means of early agricultural and non-agricultural
685 practices during the periods preceding TW14 (5700-6200 BP). It should be noted that HYDE 3.2 population
686 estimates are highly debated in the land use community due to their uncertainties related to strong
687 dependency on a few historical population sources, such as McEvedy and Jones (1978), Maddison (2001) and
688 Livi-Bacci (2007) (uncertainty ranges reported by Goldewijk et al., 2017b). However, our conclusion on partially
689 non-agricultural nature of high HPI values at Mid-Holocene is also supported by the widespread evidence of
690 hunter-gatherer land use, which indicates that land-cover were largely transformed by humans prior to
691 agricultural onset (Bos and Urz, 2003; Finsinger et al., 2006; Nikulina et al., 2022; Roebroeks et al., 2021;
692 Scherjon et al., 2015). Moreover, findings of Ellis et al. (2021), based on the analysis of spatially explicit global
693 reconstruction of historical human populations and land use, show that nearly three quarters of Earth's land
694 was already inhabited by hunter-gatherer and/or early agricultural societies at the beginning of the current
695 interglacial interval, transforming wildlands into cultured anthromes. Their conclusions are in line with our
696 findings that indicate around 70% difference between reconstructed and potential natural state of land-cover at
697 5700-6200 BP (Fig. 5, TW14). Contrastingly, KK10 land use indicates 17% of land-cover change over the
698 same study area at 5700-6200 BP (Fig. 6, right panel, TW14), which is rather an indicator for adoption of
699 agriculture, than land-cover "naturalness". Notably, high HPI values at TW14 are concentrated in the
700 Mediterranean region (see Fig. 2). In support of our findings, a synthesis of existing sedimentary charcoal
701 records (Marlon et al., 2013) reports significant fire activity during the early Holocene in the Mediterranean
702 region. While the study of Marlon et al. (2013) acknowledges that it is difficult to analyse complex fire-
703 vegetation-climate dynamics over the Mediterranean region, they suggest strong dependence of the European
704 early Holocene fire history on climate rather than human activity. However, HPI increase across the continent
705 throughout our study period aligns with fire intensity patterns in northeastern and central Europe reported by
706 Marlon et al. (2013), which during this time they hypothesise to be driven primarily by human activity. Hence,
707 alongside the use of the climate-driven baseline in our study, high charcoal index, KK10 index and long history
708 of archaeological evidence of human presence across the Mediterranean region support our findings that
709 suggest high human pressure on vegetation "naturalness" of the region and call for a more extensive analysis

710 of HPI against charcoal records. Thus, our findings do not support the hypothesis of a relatively natural land-
711 cover in the Mid-Holocene in Europe, and suggest high levels of anthropogenic modifications to vegetation
712 composition due to cumulative effect of changes introduced by early agricultural and non-agricultural activities.

713 The HPI values indicate that at TW1 (present -100 BP) nearly 87% of the studied land-cover differed from the
714 potential natural state, which accounts for changes due to agricultural activity as well as impact of non-
715 agricultural activities, accumulated throughout the long history of human-environment interaction. These values
716 are comparable with previously published estimates, indicating that from 75 to 95% of the global area is
717 somewhat transformed by human societies (Ellis et al., 2010, 2021; Williams et al., 2015). It is, however,
718 challenging to estimate the full extent of anthropogenic impact on land-cover from the existing literature, as
719 lands that are described as “natural” often exhibit long histories of use, including protected areas, managed
720 forest and cultural landscapes (Ellis et al., 2021). Using a quantitative approach, our results validated high
721 levels of cumulative anthropogenic change of vegetation cover at 6000 BP (nearly 72%) and in the modern
722 period (nearly 87%) and emphasized that while agriculture was an important driver of land-cover change in the
723 Holocene, other human practices also significantly contributed to divergence of land-cover from its natural
724 state. Similar conclusions were reported by Strona et al. (2016), who compared forest structure data with PNV
725 simulations, and indicated that at present day European forests are far from a natural condition, showing only
726 moderate signals of the ecological spatial structure typical of undisturbed vegetation (mostly at higher
727 latitudes). It should be noted that while HPI values reflect time-cumulative anthropogenic impact on
728 landscapes, they do not represent exclusively unstable or disturbed ecosystems. If, after an anthropogenic
729 disturbance, an area recovered into a stable and mature ecosystem which is different to the existing pre-
730 disturbance ecosystem, it is still considered to have been altered by human activity through our analysis.

731 Hence, our findings are not directly comparable with a concept of disturbed ecosystems used in ecology, since
732 this study quantifies magnitude by which humans shifted vegetation off its natural climate-driven course
733 regardless of the end-state of the resulting ecosystem. Our findings, however, contribute to the debate on the
734 start of Anthropocene (Lewis and Maslin, 2015; Ruddiman et al., 2016; Ruddiman, 2013, 2018; Smith and
735 Zeder, 2013; Waters et al., 2016; Zalasiewicz et al., 2021), highlighting the importance of acknowledging the
736 long history of anthropogenic land-cover modifications.

737 Conclusions

738 In this study we examined the relationship between simulated potential vegetation (PNV) and pollen-based
739 regional estimates of vegetation abundance (REVEALS) to quantify human pressure on land-cover over the
740 second half of the Holocene (6200 BP – AD 2015). With this method we observed a northward increase of
741 anthropogenic pressure in time, expressed in a form of a human pressure index (HPI) in the largest part of
742 continental Europe (41 to 54°N) throughout the second half of the Holocene. The time and location of this
743 increase coincide in trajectory and evolution with well-known anthropogenic land-cover change (ALCC)
744 scenarios, KK10 and HYDE 3.2, as well as with findings of the ArchaeoGLOBE initiative. Similar to KK10 and
745 Archaeoglobe, in the Mid-Holocene HPI values suggest anthropogenic land-cover modifications across
746 Mediterranean Europe, and partial modifications in central and northern Europe. From there, HPI extends
747 towards the north, with increasing intensity around 1200-1700 BP, following patterns similar to the ALCC
748 scenarios. Our study found that almost 60% of grid cells exhibited a significant increase in HPI values during
749 the modern time (TW1), compared to 5700-6200 BP (TW14). These findings align with estimates of ALCC:
750 nearly 56% of the study area's land-cover was transformed by human activities during the modern era (TW1)
751 based on KK10 estimates, while HYDE 3.2 estimates suggest that agriculture impacted nearly 45% of the land-
752 cover, with grazing accounting for 18% and cropland accounting for 27%. However, our inferred human impact
753 on vegetation (as indicated by HPI values) was greater than suggested by the KK10 deforestation index, and
754 HYDE 3.2 cropland and grazing estimates. We observed high initial values of HPI at 5700-6200 BP, indicating
755 up to 70% of the vegetation composition was affected by humans, as well as the absence of correlation
756 between presence of agricultural taxa in REVEALS. These findings suggest that our approach demonstrates
757 human impact on land-cover in a broader aspect than agriculture. Significant correlation of HPI with HYDE 3.2
758 population density ($r = 0.75$, $p\text{-value} < 0.005$) indicates that the HPI is strongly associated with human activity.
759 Our findings suggest that up to 70% of vegetation composition in Europe may have been affected by both early
760 agricultural and pre-agricultural human practices prior to the Mid-Holocene. In the context of the debate about
761 the chronology of the Anthropocene, this study suggests that anthropogenic land-cover change transcends the
762 boundaries of agriculture. It highlights the significance of cumulative effect of pre-agricultural practices on the
763 state of land-cover in the Mid-Holocene, and calls for a more comprehensive exploration of the complex
764 interactions between humans and the environment during that era.

765 CRediT author statement:

766 **Anhelina Zapolska:** Conceptualization, Methodology, Software, Formal analysis, Investigation, Writing -
767 Original Draft. **Maria Antonia Serge:** Investigation, Resources , Data Curation, Writing - Review & Editing.
768 **Florence Mazier:** Conceptualization, Investigation, Resources, Data Curation, Writing - Review & Editing.
769 **Aurélien Quiquet:** Software, Methodology, Writing - Review & Editing. **Hans Renssen:** Methodology,
770 Software, Writing - Review & Editing, Supervision. **Mathieu Vrac:** Software, Methodology, Writing - Review &
771 Editing. **Ralph Fyfe:** Investigation, Resources, Writing - Review & Editing. **Didier M. Roche:**
772 Conceptualization, Methodology, Software, Investigation, Writing - Original Draft, Supervision, Project
773 administration.

774

775 Acknowledgements:

776 The authors would like to thank Louis M. François for providing the CARAIB global dynamic vegetation model
777 and his help in running it. We would also like to express our sincere appreciation to Emily Vella, Kailin
778 Hatlestad, Alexandre Martinez and Anastasia Nikulina for their invaluable contributions and expertise during
779 the review process.

780

781 Funding:

782 The research is financed through the European Union's Horizon 2020 research and innovation programme
783 within the TERRANOVA project, No 813904, and supported by the Vrije Universiteit Amsterdam. The paper
784 reflects the views only of the authors, and the European Union cannot be held responsible for any use which
785 may be made of the information contained therein.

786 The study is also a contribution to the Past Global Change (PAGES) project and its working group
787 LandCover6k that in turn received support from the Swiss National Science Foundation, the Swiss Academy of
788 Sciences, the U.S. National Science Foundation, and the Chinese Academy of Sciences.

789

790 References

- 791 Archibald, S., Staver, A. C. C., and Levin, S. A.: Evolution of human-driven fire regimes in Africa, *Proc. Natl.*
792 *Acad. Sci. U. S. A.*, 109, 847–852, <https://doi.org/www.pnas.org/cgi/doi/10.1073/pnas.1118648109>, 2012.
- 793 Arthur, F., Roche, D. M., Fyfe, R., Quiquet, A., and Renssen, H.: Simulations of the Holocene Climate in
794 Europe Using Dynamical Downscaling within the iLOVECLIM model (version 1.1), *Clim. Past*,
795 <https://doi.org/https://doi.org/10.5194/cp-2022-21>, 2022.
- 796 Bartlein, P. J., Harrison, S. P., Brewer, S., Connor, S., Davis, B. A. S., Gajewski, K., Guiot, J., Harrison-
797 Prentice, T. I., Henderson, A., Peyron, O., Prentice, I. C., Scholze, M., Seppä, H., Shuman, B., Sugita, S.,
798 Thompson, R. S., Viau, A. E., Williams, J., and Wu, H.: Pollen-based continental climate reconstructions at 6
799 and 21 ka: A global synthesis, *Clim. Dyn.*, 37, 775–802, <https://doi.org/10.1007/s00382-010-0904-1>, 2011.
- 800 Bauer, A. M., Edgeworth, M., Edwards, L. E., Ellis, E. C., Gibbard, P., and Merritts, D. J.: Anthropocene: event
801 or epoch?, *Nature*, 597, 332, <https://doi.org/10.1038/D41586-021-02448-Z>, 2021.
- 802 Beaujot, R.: A Concise History of World Population, *Can. Stud. Popul.*, 41, 215,
803 <https://doi.org/10.25336/p67g81>, 2014.
- 804 Behre, K.-E.: The interpretation of anthropogenic indicators in pollen diagrams, *Cent. Natl. la Rech. Sci.*, 225–
805 245, 1981.
- 806 Berger, A. L.: Long-term variations of daily insolation and Quaternary climatic changes., *J. Atmos. Sci.*, 35,
807 2361–2367, [https://doi.org/10.1175/1520-0469\(1978\)035<2362:ltvodi>2.0.co;2](https://doi.org/10.1175/1520-0469(1978)035<2362:ltvodi>2.0.co;2), 1978.
- 808 Bos, J. A. A. A. and Urz, R.: Late Glacial and early Holocene environment in the middle Lahn river valley
809 (Hessen, central-west Germany) and the local impact of early Mesolithic people—pollen and macrofossil
810 evidence, *Veg. Hist. Archaeobot.*, 12, 19–36, <https://doi.org/10.1007/s00334-003-0006-7>, 2003.
- 811 Bouttes, N., Lhardy, F., Quiquet, A., Paillard, D., Goosse, H., and Roche, D. M.: Deglacial climate changes as
812 forced by ice sheet reconstructions, *EGU Sph. Prepr.*, <https://doi.org/10.5194/egusphere-2022-993>, 2023.
- 813 Braje, T. J. and Erlandson, J. M.: Human acceleration of animal and plant extinctions: A Late Pleistocene,
814 Holocene, and Anthropocene continuum, *Anthropocene*, 4, 14–23,
815 <https://doi.org/10.1016/J.ANCENE.2013.08.003>, 2013a.

816 Braje, T. J. and Erlandson, J. M.: Looking forward, looking back: Humans, anthropogenic change, and the
817 Anthropocene, *Anthropocene*, 4, 116–121, <https://doi.org/10.1016/j.ancene.2014.05.002>, 2013b.

818 Brovkin, V., Ganopolski, A., and Svirezhev, Y.: A continuous climate-vegetation classification for use in
819 climate-biosphere studies, *Ecol. Modell.*, 101, 251–261, [https://doi.org/10.1016/S0304-3800\(97\)00049-5](https://doi.org/10.1016/S0304-3800(97)00049-5), 1997.

820 Carracedo, V., Cunill, R., García-Codron, J. C., Pèlach, A., Pérez-Obiol, R., and Soriano, J. M.: History of
821 fires and vegetation since the Neolithic in the Cantabrian Mountains (Spain), *L. Degrad. Dev.*, 29, 2060–2072,
822 <https://doi.org/10.1002/LDR.2891>, 2018.

823 Certini, G. and Scalenghe, R.: Anthropogenic soils are the golden spikes for the Anthropocene, *Holocene*, 21,
824 1269–1274,
825 https://doi.org/10.1177/0959683611408454/ASSET/IMAGES/LARGE/10.1177_0959683611408454-
826 [FIG2.JPG](https://doi.org/10.1177/0959683611408454/ASSET/IMAGES/LARGE/10.1177_0959683611408454-FIG2.JPG), 2011.

827 Connor, S. E., Vannièrè, B., Colombaroli, D., Anderson, R. S., Carrión, J. S., Ejarque, A., Gil Romera, G.,
828 González-Sampériz, P., Hofer, D., Morales-Molino, C., Revelles, J., Schneider, H., van der Knaap, W. O., van
829 Leeuwen, J. F. N., and Woodbridge, J.: Humans take control of fire-driven diversity changes in Mediterranean
830 Iberia’s vegetation during the mid–late Holocene, *Holocene*, 29, 886–901,
831 <https://doi.org/10.1177/0959683619826652>, 2019.

832 Crutzen, P. J.: The “anthropocene,” *J. Phys. IV*, 12, 1–5, <https://doi.org/10.1051/JP4:20020447>, 2002.

833 Cruz-Silva, E., Harrison, S. P., Marinova, E., and Prentice, I. C.: A new method based on surface-sample
834 pollen data for reconstructing palaeovegetation patterns, *J. Biogeogr.*, 49, 1381–1396,
835 <https://doi.org/10.1111/JBI.14448>, 2022.

836 Dallmeyer, A., Claussen, M., and Brovkin, V.: Harmonising plant functional type distributions for evaluating
837 Earth system models, *Clim. Past*, 15, 335–366, <https://doi.org/10.5194/cp-15-335-2019>, 2019.

838 Dallmeyer, A., Poska, A., Marquer, L., Seim, A., and Gaillard-Lemdahl, M.-J.: The challenge of comparing
839 pollen-based quantitative vegetation reconstructions with outputs from vegetation models – a European
840 perspective, *Clim. Past Discuss.*, 1–50, <https://doi.org/10.5194/CP-2023-16>, 2023.

841 Deza-Araujo, M., Morales-Molino, C., Tinner, W., Henne, P. D., Heitz, C., Pezzatti, G. B., Hafner, A., and

842 Conedera, M.: A critical assessment of human-impact indices based on anthropogenic pollen indicators, *Quat.*
843 *Sci. Rev.*, 236, 106291, <https://doi.org/10.1016/J.QUASCIREV.2020.106291>, 2020.

844 Deza-Araujo, M., Morales-Molino, C., Conedera, M., Henne, P. D., Krebs, P., Hinz, M., Heitz, C., Hafner, A.,
845 and Tinner, W.: A new indicator approach to reconstruct agricultural land use in Europe from sedimentary
846 pollen assemblages, *Palaeogeogr. Palaeoclimatol. Palaeoecol.*, 599, 111051,
847 <https://doi.org/10.1016/J.PALAEO.2022.111051>, 2022.

848 Dietze, E., Theuerkauf, M., Bloom, K., Brauer, A., Dörfler, W., Feeser, I., Feurdean, A., Gedminienė, L.,
849 Giesecke, T., Jahns, S., Karpińska-Kołaczek, M., Kołaczek, P., Lamentowicz, M., Latałowa, M., Marcisz, K.,
850 Obremaska, M., Pędziszewska, A., Poska, A., Rehfeld, K., Stančikaitė, M., Stivrins, N., Święta-Musznicka, J.,
851 Szal, M., Vassiljev, J., Veski, S., Wacnik, A., Weisbrodt, D., Wiethold, J., Vannièrè, B., Słowiński, M., Dörfler,
852 W., Feeser, I., Feurdean, A., Gedminiene, L., Giesecke, T., Jahns, S., Karpińska-Kołaczek, M., Kołaczek, P.,
853 Lamentowicz, M., Latałowa, M., Marcisz, K., Obremaska, M., Pędziszewska, A., Poska, A., Rehfeld, K.,
854 Stančikaite, M., Stivrins, N., Święta-Musznicka, J., Szal, M., Vassiljev, J., Veski, S., Wacnik, A., Weisbrodt, D.,
855 Wiethold, J., Vannièrè, B., and Słowiński, M.: Holocene fire activity during low-natural flammability periods
856 reveals scale-dependent cultural human-fire relationships in Europe, *Quat. Sci. Rev.*, 201, 44–56,
857 <https://doi.org/https://doi.org/10.1016/j.quascirev.2018.10.005>, 2018.

858 Doughty, C. E.: Preindustrial human impacts on global and regional environment, *Annu. Rev. Environ. Resour.*,
859 38, 503–527, <https://doi.org/10.1146/annurev-environ-032012-095147>, 2013.

860 Dury, M., Hambuckers, A., Warnant, P., Henrot, A., Favre, E., Ouberdous, M., and François, L.: Responses of
861 European forest ecosystems to 21st century climate: Assessing changes in interannual variability and fire
862 intensity, *IForest*, 4, 82–99, <https://doi.org/10.3832/ifor0572-004>, 2011.

863 Edgeworth, M., Richter, D. D. B., Waters, C., Haff, P., Neal, C., and Price, S. J.: Diachronous beginnings of the
864 anthropocene: The lower bounding surface of anthropogenic deposits, *Anthr. Rev.*, 2, 33–58,
865 https://doi.org/10.1177/2053019614565394/ASSET/IMAGES/LARGE/10.1177_2053019614565394-
866 [FIG2.JPG](https://doi.org/10.1177/2053019614565394/ASSET/IMAGES/LARGE/10.1177_2053019614565394-FIG2.JPG), 2015.

867 Edwards, L. E., Edgeworth, M., Ellis, E. C., and Leonard Gibbard, P.: The Anthropocene serves science better
868 as an event, rather than an epoch The analysis of the topographic signature of anthropogenic geomorphic

869 processes View project Continental Shelves, Drowned Landscapes, North Sea Palaeogeography View project,
870 Artic. J. Quat. Sci., <https://doi.org/10.1002/jqs.3475>, 2022.

871 Ellis, E. C., Goldewijk, K. K., Siebert, S., Lightman, D., and Ramankutty, N.: Anthropogenic transformation of
872 the biomes, 1700 to 2000, *Glob. Ecol. Biogeogr.*, 19, 589–606, 2010.

873 Ellis, E. C., Kaplan, J. O., Fuller, D. Q., Vavrus, S., Goldewijk, K. K., and Verburg, P. H.: Used planet: A global
874 history, <https://doi.org/10.1073/pnas.1217241110>, 14 May 2013.

875 Ellis, E. C., Gauthier, N., Goldewijk, K. K., Bird, R. B., Boivin, N., Díaz, S., Fuller, D. Q., Gill, J. L., Kaplan, J.
876 O., Kingston, N., Locke, H., McMichael, C. N. H. H., Ranco, D., Rick, T. C., Rebecca Shaw, M., Stephens, L.,
877 Svenning, J. C., and Watson, J. E. M. M.: People have shaped most of terrestrial nature for at least 12,000
878 years, *Proc. Natl. Acad. Sci. U. S. A.*, 118, 1–8, <https://doi.org/10.1073/pnas.2023483118>, 2021.

879 Erlandson, J. M. and Braje, T. J.: Archeology and the anthropocene, *Anthropocene*, 4, 1–7,
880 <https://doi.org/10.1016/j.ancene.2014.05.003>, 2013.

881 FAO: FAO publications catalogue 2022, FAO, Rome, Italy, <https://doi.org/10.4060/cc2323en>, 2022.

882 Farris, E., Filibeck, G., Marignani, M., and Rosati, L.: The power of potential natural vegetation (and of spatial-
883 temporal scale): a response to Carrión & Fernández (2009), *J. Biogeogr.*, 37, 2211–2213,
884 <https://doi.org/10.1111/J.1365-2699.2010.02323.X>, 2010.

885 Finsinger, W., Tinner, W., Van Der Knaap, W. O., and Ammann, B.: The expansion of hazel (*Corylus avellana*
886 L.) in the southern Alps: a key for understanding its early Holocene history in Europe?, *Quat. Sci. Rev.*, 25,
887 612–631, <https://doi.org/10.1016/J.QUASCIREV.2005.05.006>, 2006.

888 Foley, S. F., Gronenborn, D., Andreae, M. O., Kadereit, J. W., Esper, J., Scholz, D., Pöschl, U., Jacob, D. E.,
889 Schöne, B. R., Schreg, R., Vött, A., Jordan, D., Lelieveld, J., Weller, C. G., Alt, K. W., Gaudzinski-Windheuser,
890 S., Bruhn, K. C., Tost, H., Sirocko, F., and Crutzen, P. J.: The Palaeoanthropocene – The beginnings of
891 anthropogenic environmental change, *Anthropocene*, 3, 83–88,
892 <https://doi.org/10.1016/J.ANCENE.2013.11.002>, 2013.

893 François, L. M., Delire, C., Warnant, P., and Munhoven, G.: Modelling the glacial-interglacial changes in the
894 continental biosphere, *Glob. Planet. Change*, 16–17, 37–52, [https://doi.org/10.1016/S0921-8181\(98\)00005-8](https://doi.org/10.1016/S0921-8181(98)00005-8),

895 1998.

896 François, L. M., Utescher, T., Favre, E., Henrot, A. J., Warnant, P., Micheels, A., Erdei, B., Suc, J. P.,
897 Cheddadi, R., and Mosbrugger, V.: Modelling Late Miocene vegetation in Europe: Results of the CARAIB
898 model and comparison with palaeovegetation data, *Palaeogeogr. Palaeoclimatol. Palaeoecol.*, 304, 359–378,
899 <https://doi.org/10.1016/J.PALAEO.2011.01.012>, 2011.

900 Fyfe, R. M., Twiddle, C., Sugita, S., Gaillard, M.-J., Barratt, P., Caseldine, C. J., Dodson, J., Edwards, K. J.,
901 Farrell, M., Froyd, C., Grant, M. J., Huckerby, E., Innes, J. B., Shaw, H., and Waller, M.: The Holocene
902 vegetation cover of Britain and Ireland: Overcoming problems of scale and discerning patterns of openness,
903 *Quat. Sci. Rev.*, 73, 132–148, <https://doi.org/10.1016/j.quascirev.2013.05.014>, 2013.

904 Fyfe, R. M., Woodbridge, J., and Roberts, N.: From forest to farmland: Pollen-inferred land cover change
905 across Europe using the pseudobiomization approach, *Glob. Chang. Biol.*, 21, 1197–1212,
906 <https://doi.org/10.1111/GCB.12776>, 2015.

907 Fyfe, R. M., Woodbridge, J., Palmisano, A., Bevan, A., Shennan, S., Burjachs, F., Legarra Herrero, B., García
908 Puchol, O., Carrión, J. S., Revelles, J., and Roberts, C. N.: Prehistoric palaeodemographics and regional land
909 cover change in eastern Iberia, *Holocene*, 29, 799–815,
910 [https://doi.org/10.1177/0959683619826643/ASSET/IMAGES/LARGE/10.1177_0959683619826643-](https://doi.org/10.1177/0959683619826643/ASSET/IMAGES/LARGE/10.1177_0959683619826643-FIG6.JPEG)
911 [FIG6.JPEG](https://doi.org/10.1177/0959683619826643/ASSET/IMAGES/LARGE/10.1177_0959683619826643-FIG6.JPEG), 2019.

912 Gaillard, M.-J.: POLLEN METHODS AND STUDIES | Archaeological Applications, *Encycl. Quat. Sci.*, 2570–
913 2595, <https://doi.org/10.1016/B0-44-452747-8/00214-3>, 2007.

914 Gaillard, M.-J.: Pollen Methods and Studies. Archaeological Applications, in: *Encyclopedia of Quaternary*
915 *Science: Second Edition*, edited by: Elias, S. and Mock, C. J., Elsevier, Amsterdam, 880–904,
916 <https://doi.org/10.1016/B978-0-444-53643-3.00182-5>, 2013.

917 Gaillard, M.-J., Sugita, S., Mazier, F., Trondman, A. K., Broström, A., Hickler, T., Kaplan, J. O., Kjellström, E.,
918 Kokfelt, U., Kuneš, P., Lemmen, C., Miller, P., Olofsson, J., Poska, A., Rundgren, M., Smith, B., Strandberg,
919 G., Fyfe, R., Nielsen, A. B., Alenius, T., Balakauskas, L., Barnekow, L., Birks, H. J. B., Bjune, A., Björkman, L.,
920 Giesecke, T., Hjelle, K., Kalnina, L., Kangur, M., Van Der Knaap, W. O., Koff, T., Lageras, P., Latałowa, M.,

921 Leydet, M., Lechterbeck, J., Lindbladh, M., Odgaard, B., Peglar, S., Segerström, U., Von Stedingk, H., and
922 Seppä, H.: Holocene land-cover reconstructions for studies on land cover-climate feedbacks, *Clim. Past*, 6,
923 483–499, <https://doi.org/10.5194/cp-6-483-2010>, 2010.

924 Gibbard, P., Walker, M., Bauer, A., Edgeworth, M., Edwards, L., Ellis, E., Finney, S., Gill, J. L., Maslin, M.,
925 Merritts, D., and Ruddiman, W.: The Anthropocene as an Event, not an Epoch, *J. Quat. Sci.*, 37, 395–399,
926 <https://doi.org/10.1002/JQS.3416>, 2022.

927 Githumbi, E., Fyfe, R., Gaillard, M.-J., Trondman, A. K., Mazier, F., Nielsen, A. B., Poska, A., Sugita, S.,
928 Woodbridge, J., Azuara, J., Feurdean, A., Grindean, R., Lebreton, V., Marquer, L., Nebout-Combourieu, N.,
929 Stančikaite, M., Tanțău, I., Tonkov, S., Shumilovskikh, L., Åkesson, C., Balakauskas, L., Batalova, V., Birks, H.
930 J. B., Bjune, A. E., Borisova, O., Bozilova, E., Burjachs, F., Cheddadi, R., Christiansen, J., David, R., De Klerk,
931 P., Di Rita, F., Dörfler, W., Doyen, E., Eastwood, W., Etienne, D., Feeser, I., Filipova-Marinova, M., Fischer, E.,
932 Galop, D., Carrion, J. G. S., Gauthier, E., Giesecke, T., Herking, C., Herzsuh, U., Jouffroy-Bapicot, I.,
933 Kasianova, A., Kouli, K., Kuneš, P., Lagerås, P., Latalowa, M., Lechterbeck, J., Leroyer, C., Leydet, M.,
934 Lisytstina, O., Lukanina, E., Magyari, E., Marguerie, D., Lippi, M. M., Mensing, S., Mercuri, A. M., Miebach, A.,
935 Milburn, P., Miras, Y., Del Molino, C. M., Mrotzek, A., Nosova, M., Odgaard, B. V., Overballe-Petersen, M.,
936 Panajiotidis, S., Pavlov, D., Persson, T., Pinke, Z., Ruffaldi, P., Sapelko, T., Schmidt, M., Schult, M., Stivrins,
937 N., Tarasov, P. E., Theuerkauf, M., Veski, S., Wick, L., Wiethold, J., Woldring, H., and Zernitskaya, V.:
938 European pollen-based REVEALS land-cover reconstructions for the Holocene: Methodology, mapping and
939 potentials, *Earth Syst. Sci. Data*, 14, 1581–1619, <https://doi.org/10.5194/ESSD-14-1581-2022>, 2022.

940 Goldewijk, K. K., Beusen, A., and Janssen, P.: Long-term dynamic modeling of global population and built-up
941 area in a spatially explicit way: HYDE 3.1, *Holocene*, 20, 565–573, 2010.

942 Goldewijk, K. K., Beusen, A., Van Drecht, G., and De Vos, M.: The HYDE 3.1 spatially explicit database of
943 human-induced global land-use change over the past 12,000 years, *Glob. Ecol. Biogeogr.*, 20, 73–86,
944 <https://doi.org/10.1111/j.1466-8238.2010.00587.x>, 2011.

945 Goldewijk, K. K., Beusen, A., Doelman, J., and Stehfest, E.: Anthropogenic land use estimates for the
946 Holocene - HYDE 3.2, *Earth Syst. Sci. Data*, 9, 927–953, <https://doi.org/10.5194/essd-9-927-2017>, 2017a.

947 Goldewijk, K. K., Dekker, S. C., and van Zanden, J. L.: Per-capita estimations of long-term historical land use

948 and the consequences for global change research, *J. Land Use Sci.*, 12, 313–337,
949 <https://doi.org/10.1080/1747423X.2017.1354938>, 2017b.

950 Goosse, H. and Fichefet, T.: Importance of ice-ocean interactions for the global ocean circulation: A model
951 study, *J. Geophys. Res. Ocean.*, 104, 23337–23355, <https://doi.org/10.1029/1999jc900215>, 1999.

952 Goosse, H., Brovkin, V., Fichefet, T., Haarsma, R., Huybrechts, P., Jongma, J., Mouchet, A., Selten, F.,
953 Barriat, P. Y., Campin, J. M., Deleersnijder, E., Driesschaert, E., Goelzer, H., Janssens, I., Loutre, M. F.,
954 Morales Maqueda, M. A., Opsteegh, T., Mathieu, P. P., Munhoven, G., Pettersson, E. J., Renssen, H., Roche,
955 D. M., Schaeffer, M., Tartinville, B., Timmermann, A., and Weber, S. L.: Description of the Earth system model
956 of intermediate complexity LOVECLIM version 1.2, *Geosci. Model Dev.*, 3, 603–633,
957 <https://doi.org/10.5194/GMD-3-603-2010>, 2010.

958 Gronenborn, D. and Horejs, B.: Expansion of farming in western Eurasia, 9600 - 4000 cal BC (update vers.
959 2021.2), Zenodo, <https://doi.org/10.5281/ZENODO.5903165>, 2021.

960 Harrison, S. P., Gaillard, M.-J., Stocker, B. D., Vander Linden, M., Klein Goldewijk, K., Boles, O., Braconnot,
961 P., Dawson, A., Fluet-Chouinard, E., Kaplan, J. O., Kastner, T., Pausata, F. S. R., Robinson, E., Whitehouse,
962 N. J., Madella, M., Morrison, K. D., Goldewijk, K. K., Boles, O., Braconnot, P., Dawson, A., Fluet-Chouinard, E.,
963 Kaplan, J. O., Kastner, T., Pausata, F. S. R., Robinson, E., Whitehouse, N. J., Madella, M., and Morrison, K.
964 D.: Development and testing scenarios for implementing land use and land cover changes during the Holocene
965 in Earth system model experiments, *Geosci. Model Dev.*, 13, 805–824, [https://doi.org/10.5194/GMD-13-805-](https://doi.org/10.5194/GMD-13-805-2020)
966 2020, 2020.

967 Head, M. J., Steffen, W., Fagerlind, D., Waters, C. N., Poirier, C., Syvitski, J., Zalasiewicz, J. A., Barnosky, A.
968 D., Cearreta, A., Jeandel, C., Leinfelder, R., McNeill, J. R., Rose, N. L., Summerhayes, C., Wagnreich, M., and
969 Zinke, J.: The Great Acceleration is real and provides a quantitative basis for the proposed Anthropocene
970 Series/Epoch, *Episodes J. Int. Geosci.*, 45, 359–376, <https://doi.org/10.18814/EPIIUGS/2021/021031>, 2022a.

971 Head, M. J., Zalasiewicz, J. A., Waters, C. N., Turner, S. D., Williams, M., Barnosky, A. D., Steffen, W.,
972 Wagnreich, M., Haff, P. K., Syvitski, J., Leinfelder, R., Mccarthy, F. M. G., Rose, N. L., Wing, S. L., An, Z.,
973 Cearreta, A., Cundy, A. B., Fairchild, I. J., Han, Y., Ivar Do Sul, J. A., Jeandel, C., McNeill, J. R., and
974 Summerhayes, C. P.: The proposed Anthropocene Epoch/Series is underpinned by an extensive array of mid-

975 20th century stratigraphic event signals, *J. Quat. Sci.*, 37, 1181–1187, <https://doi.org/10.1002/JQS.3467>,
976 2022b.

977 Hengl, T., Walsh, M. G., Sanderman, J., Wheeler, I., Harrison, S. P., and Prentice, I. C.: Global mapping of
978 potential natural vegetation: An assessment of machine learning algorithms for estimating land potential,
979 *PeerJ*, 2018, <https://doi.org/10.7717/peerj.5457>, 2018.

980 Henrot, A. J., Utescher, T., Erdei, B., Dury, M., Hamon, N., Ramstein, G., Krapp, M., Herold, N., Goldner, A.,
981 Favre, E., Munhoven, G., and François, L.: Middle Miocene climate and vegetation models and their validation
982 with proxy data, *Palaeogeogr. Palaeoclimatol. Palaeoecol.*, 467, 95–119,
983 <https://doi.org/10.1016/j.palaeo.2016.05.026>, 2017.

984 Hiscock, P. and Attenbrow, V.: Dates and demography? The need for caution in using radiometric dates as a
985 robust proxy for prehistoric population change, *Archaeol. Ocean.*, 51, 218–219,
986 <https://doi.org/10.1002/ARCO.5096>, 2016.

987 Jackson, S. T.: Natural, potential and actual vegetation in North America, *J. Veg. Sci.*, 24, 772–776,
988 <https://doi.org/10.1111/JVS.12004>, 2013.

989 Kalis, A. J., Merkt, J., and Wunderlich, J.: Environmental changes during the Holocene climatic optimum in
990 central Europe - human impact and natural causes, *Quat. Sci. Rev.*, 22, 33–79, <https://doi.org/10.1016/S0277->
991 [3791\(02\)00181-6](https://doi.org/10.1016/S0277-3791(02)00181-6), 2003.

992 Kaplan, J. O. and Krumhardt, K. M.: The KK10 Anthropogenic Land Cover Change scenario for the
993 preindustrial Holocene, *PANGAEA*, <https://doi.org/10.1594/PANGAEA.871369>, 2011.

994 Kaplan, J. O., Krumhardt, K. M., and Zimmermann, N.: The prehistoric and preindustrial deforestation of
995 Europe, *Quat. Sci. Rev.*, 28, 3016–3034, <https://doi.org/10.1016/j.quascirev.2009.09.028>, 2009.

996 Kaplan, J. O., Krumhardt, K. M., Ellis, E. C., Ruddiman, W. F., Lemmen, C., and Goldewijk, K. K.: Holocene
997 carbon emissions as a result of anthropogenic land cover change, *Holocene*, 21, 775–791,
998 <https://doi.org/10.1177/0959683610386983>, 2011.

999 Kaplan, J. O., Krumhardt, K. M., Gaillard, M.-J., Sugita, S., Trondman, A.-K. K., Fyfe, R., Marquer, L., Mazier,
000 F., and Nielsen, A. B.: Constraining the deforestation history of Europe: Evaluation of historical land use

001 scenarios with pollen-based land cover reconstructions, *Land*, 6, 91, <https://doi.org/10.3390/land6040091>,
002 2017.

003 Koch, P. L. and Barnosky, A. D.: Late Quaternary Extinctions: State of the Debate,
004 <https://doi.org/10.1146/annurev.ecolsys.34.011802.132415>, 37, 215–250,
005 <https://doi.org/10.1146/ANNUREV.ECOLSYS.34.011802.132415>, 2006.

006 Kuosmanen, N., Marquer, L., Tallavaara, M., Molinari, C., Zhang, Y., Alenius, T., Edinborough, K., Pesonen,
007 P., Reitalu, T., Renssen, H., Trondman, A. K., and Seppä, H.: The role of climate, forest fires and human
008 population size in Holocene vegetation dynamics in Fennoscandia, *J. Veg. Sci.*, 29, 382–392, 2018.

009 Lange, S.: Earth2Observe, WFDEI and ERA-Interim data Merged and Bias-corrected for ISIMIP (EWEMBI),
010 GFZ Data Serv., 2016.

011 Laurent, J. M., François, L. M., Bar-Hen, A., Bel, L., and Cheddadi, R.: European bioclimatic affinity groups:
012 Data-model comparisons, *Glob. Planet. Change*, 61, 28–40, <https://doi.org/10.1016/j.gloplacha.2007.08.017>,
013 2008.

014 Lechterbeck, J., Edinborough, K., Kerig, T., Fyfe, R., Roberts, N., and Shennan, S.: Is Neolithic land use
015 correlated with demography? An evaluation of pollen-derived land cover and radiocarbon-inferred demographic
016 change from Central Europe, *Holocene*, 24, 1297–1307,
017 https://doi.org/10.1177/0959683614540952/ASSET/IMAGES/LARGE/10.1177_0959683614540952-
018 [FIG4.JPEG](#), 2014.

019 Lemmen, C.: World distribution of land cover changes during Pre-and Protohistoric Times and estimation of
020 induced carbon releases, *Geoarchaeology human-environment Connect.*, 15, 303–312,
021 <https://doi.org/10.4000/geomorphologie.7756>, 2009.

022 Levavasseur, G., Vrac, M., Roche, D. M., and Paillard, D.: Statistical modelling of a new global potential
023 vegetation distribution, *Environ. Res. Lett.*, 7, 44019–44030, <https://doi.org/10.1088/1748-9326/7/4/044019>,
024 2012.

025 Levavasseur, G., Vrac, M., Roche, D. M., Paillard, D., and Guiot, J.: An objective methodology for potential
026 vegetation reconstruction constrained by climate, *Glob. Planet. Change*, 104, 7–22,

027 <https://doi.org/10.1016/J.GLOPLACHA.2013.01.008>, 2013.

028 Lewis, S. L. and Maslin, M. A.: Defining the Anthropocene, *Nat.* 2015 5197542, 519, 171–180,
029 <https://doi.org/10.1038/nature14258>, 2015.

030 Lightfoot, K. G. and Cuthrell, R. Q.: Anthropogenic burning and the Anthropocene in late-Holocene California,
031 *Holocene*, 25, 1581–1587, <https://doi.org/10.1177/0959683615588376>, 2015.

032 Loidi, J., del Arco, M., Pérez de Paz, P. L., Asensi, A., Díez Garretas, B., Costa, M., Díaz González, T.,
033 Fernández-González, F., Izco, J., Penas, A., Rivas-Martínez, S., and Sánchez-Mata, D.: Understanding
034 properly the 'potential natural vegetation' concept, *J. Biogeogr.*, 37, 2209–2211,
035 <https://doi.org/10.1111/J.1365-2699.2010.02302.X>, 2010.

036 Maddison, A.: *The World Economy*, OECD, Paris, France, <https://doi.org/10.1787/9789264189980-EN>, 2001.

037 Mann, D. H., Groves, P., Gaglioti, B. V., and Shapiro, B. A.: Climate-driven ecological stability as a globally
038 shared cause of Late Quaternary megafaunal extinctions: the Plaids and Stripes Hypothesis, *Biol. Rev.*, 94,
039 328–352, <https://doi.org/10.1111/BRV.12456>, 2019.

040 Marlon, J. R., Bartlein, P. J., Danialu, A. L., Harrison, S. P., Maezumi, S. Y., Power, M. J., Tinner, W., and
041 Vanniére, B.: Global biomass burning: a synthesis and review of Holocene paleofire records and their controls,
042 *Quat. Sci. Rev.*, 65, 5–25, <https://doi.org/10.1016/J.QUASCIREV.2012.11.029>, 2013.

043 Marquer, L., Gaillard, M.-J., Sugita, S., Trondman, A. K., Mazier, F., Nielsen, A. B., Fyfe, R. M., Odgaard, B.
044 V., Alenius, T., Birks, H. J. B., Bjune, A. E., Christiansen, J., Dodson, J., Edwards, K. J., Giesecke, T.,
045 Herzschuh, U., Kangur, M., Lorenz, S., Poska, A., Schult, M., and Seppä, H.: Holocene changes in vegetation
046 composition in northern Europe: why quantitative pollen-based vegetation reconstructions matter, *Quat. Sci.*
047 *Rev.*, 90, 199–216, <https://doi.org/10.1016/J.QUASCIREV.2014.02.013>, 2014.

048 Marquer, L., Gaillard, M.-J., Sugita, S., Poska, A., Trondman, A. K., Mazier, F., Nielsen, A. B., Fyfe, R. M.,
049 Jönsson, A. M., Smith, B., Kaplan, J. O., Alenius, T., Birks, H. J. B., Bjune, A. E., Christiansen, J., Dodson, J.,
050 Edwards, K. J., Giesecke, T., Herzschuh, U., Kangur, M., Koff, T., Latałowa, M., Lechterbeck, J., Olofsson, J.,
051 and Seppä, H.: Quantifying the effects of land use and climate on Holocene vegetation in Europe, *Quat. Sci.*
052 *Rev.*, 171, 20–37, 2017.

053 Mazier, F., Galop, D., Brun, C., and Buttler, A.: Modern pollen assemblages from grazed vegetation in the
054 western Pyrenees, France: A numerical tool for more precise reconstruction of past cultural landscapes, *The*
055 *Holocene*, 16, 91–103, <https://doi.org/10.1191/0959683606hl908rp>, 2006.

056 Mazier, F., Galop, D., Gaillard, M.-J., Rendu, C., Cugny, C., Legaz, A., Peyron, O., and Buttler, A.:
057 Multidisciplinary approach to reconstructing local pastoral activities: An example from the Pyrenean Mountains
058 (Pays Basque), *Holocene*, 19, 171–188, <https://doi.org/10.1177/0959683608098956>, 2009.

059 Mazier, F., Gaillard, M.-J., Kuneš, P., Sugita, S., Trondman, A. K., and Broström, A.: Testing the effect of site
060 selection and parameter setting on REVEALS-model estimates of plant abundance using the Czech
061 Quaternary Palynological Database, *Rev. Palaeobot. Palynol.*, 187, 38–49,
062 <https://doi.org/10.1016/j.revpalbo.2012.07.017>, 2012.

063 McEvedy, C. and Jones, R.: *Atlas of world population history*, Penguin Books Ltd, Northwestern University,
064 Hammondsorth, UK, 1–368 pp., 1978.

065 McWethy, D. B., Whitlock, C., Wilmshurst, J. M., McGlone, M. S., Fromont, M., Li, X., Dieffenbacher-Krall, A.,
066 Hobbs, W. O., Fritz, S. C., and Cook, E. R.: Rapid landscape transformation in South Island, New Zealand,
067 following initial Polynesian settlement, *Proc. Natl. Acad. Sci. U. S. A.*, 107, 21343–21348,
068 https://doi.org/10.1073/PNAS.1011801107/SUPPL_FILE/PNAS.1011801107_SI.PDF, 2010.

069 Mercuri, A. M., Bandini Mazzanti, M., Florenzano, A., Montecchi, M. C., and Rattighieri, E.: *Olea*, *Juglans* and
070 *Castanea*: The OJC group as pollen evidence of the development of human-induced environments in the
071 Italian peninsula, *Quat. Int.*, 303, 24–42, <https://doi.org/10.1016/J.QUAINT.2013.01.005>, 2013.

072 Morrison, K. D., Hammer, E., Boles, O., Madella, M., Whitehouse, N., Gaillard, M. J., Bates, J., Linden, M.
073 Vander, Merlo, S., Yao, A., Popova, L., Hill, A. C., Antolin, F., Bauer, A., Biagetti, S., Bishop, R. R., Buckland,
074 P., Cruz, P., Dreslerová, D., Dusseldorp, G., Ellis, E., Filipovic, D., Foster, T., Hannaford, M. J., Harrison, S. P.,
075 Hazarika, M., Herold, H., Hilpert, J., Kaplan, J. O., Kay, A., Goldewijk, K. K., Kolár, J., Kyazike, E., Laabs, J.,
076 Lancelotti, C., Lane, P., Lawrence, D., Lewis, K., Lombardo, U., Lucarini, G., Arroyo-Kalin, M., Marchant, R.,
077 Mayle, F., McClatchie, M., McLeester, M., Mooney, S., Moskal-Del Hoyo, M., Navarrete, V., Ndiema, E.,
078 Neves, E. G., Nowak, M., Out, W. A., Petrie, C., Phelps, L. N., Pinke, Z., Rostain, S., Russell, T., Sluyter, A.,
079 Styring, A. K., Tamanaha, E., Thomas, E., Veerasamy, S., Welton, L., and Zanon, M.: Mapping past human

080 land use using archaeological data: A new classification for global land use synthesis and data harmonization,
081 PLoS One, 16, e0246662, <https://doi.org/10.1371/JOURNAL.PONE.0246662>, 2021.

082 Mottl, O., Flantua, S. G. A., Bhatta, K. P., Felde, V. A., Giesecke, T., Simon Goring, Grimm, E. C., Haberle, S.,
083 Hooghiemstra, H., Ivory, S., Kuneš, P., Wolters, S., Seddon, A. W. R., and Williams, J. W.: Global acceleration
084 in rates of vegetation change over the past 18,000 years, *Science (80-.)*, 372, 860–864,
085 https://doi.org/10.1126/SCIENCE.ABG1685/SUPPL_FILE/ABG1685_MOTTTL_SM.PDF, 2021.

086 Nielsen, A. B., Giesecke, T., Theuerkauf, M., Feeser, I., Behre, K. E., Beug, H. J., Chen, S. H., Christiansen,
087 J., Dörfler, W., Endtmann, E., Jahns, S., de Klerk, P., Köhl, N., Latalowa, M., Odgaard, B. V., Rasmussen, P.,
088 Stockholm, J. R., Voigt, R., Wiethold, J., and Wolters, S.: Quantitative reconstructions of changes in regional
089 openness in north-central Europe reveal new insights into old questions, *Quat. Sci. Rev.*, 47, 131–149,
090 <https://doi.org/10.1016/j.quascirev.2012.05.011>, 2012.

091 Nikulina, A., MacDonald, K., Scherjon, F., A. Pearce, E., Davoli, M., Svenning, J. C., Vella, E., Gaillard, M.-J.,
092 Zapolska, A., Arthur, F., Martinez, A., Hatlestad, K., Mazier, F., Serge, M. A., Lindholm, K. J., Fyfe, R.,
093 Renssen, H., Roche, D. M., Kluiving, S., and Roebroeks, W.: Tracking Hunter-Gatherer Impact on Vegetation
094 in Last Interglacial and Holocene Europe: Proxies and Challenges, *J. Archaeol. Method Theory*, 29, 989–1033,
095 <https://doi.org/10.1007/s10816-021-09546-2>, 2022.

096 O’Dwyer, R., Marquer, L., Trondman, A. K., and Jönsson, A. M.: Spatially Continuous Land-Cover
097 Reconstructions Through the Holocene in Southern Sweden, *Ecosystems*, 24, 1450–1467,
098 <https://doi.org/10.1007/S10021-020-00594-5/FIGURES/7>, 2021.

099 Olofsson, J. and Hickler, T.: Effects of human land-use on the global carbon cycle during the last 6,000 years,
100 in: *Vegetation History and Archaeobotany*, 605–615, <https://doi.org/10.1007/s00334-007-0126-6>, 2008.

101 Opsteegh, J. D., Haarsma, R. J., Selten, F. M., and Kattenberg, A.: ECBILT: A dynamic alternative to mixed
102 boundary conditions in ocean models, *Tellus, Ser. A Dyn. Meteorol. Oceanogr.*, 50, 348–367,
103 <https://doi.org/10.3402/tellusa.v50i3.14524>, 1998.

104 Otto, D., Rasse, D., Kaplan, J., Warnant, P., and François, L.: Biospheric carbon stocks reconstructed at the
105 Last Glacial Maximum: Comparison between general circulation models using prescribed and computed sea

106 surface temperatures, *Glob. Planet. Change*, 33, 117–138, [https://doi.org/10.1016/S0921-8181\(02\)00066-8](https://doi.org/10.1016/S0921-8181(02)00066-8),
107 2002.

108 Pinter, N., Fiedel, S., Keeley, J. E., Pinter, N., Fiedel, S., and Keeley, J. E.: Fire and vegetation shifts in the
109 Americas at the vanguard of Paleoindian migration, *QSRv*, 30, 269–272,
110 <https://doi.org/10.1016/J.QUASCIREV.2010.12.010>, 2011.

111 Pirzamanbein, B. and Lindström, J.: Reconstruction of past human land use from pollen data and
112 anthropogenic land cover changes, *Environmetrics*, 33, e2743, <https://doi.org/10.1002/ENV.2743>, 2022.

113 Pongratz, J., Reick, C., Raddatz, T., and Claussen, M.: A reconstruction of global agricultural areas and land
114 cover for the last millennium, *Global Biogeochem. Cycles*, 22, n/a-n/a, <https://doi.org/10.1029/2007GB003153>,
115 2008.

116 Pongratz, J., Reick, C. H., Raddatz, T., and Claussen, M.: Biogeophysical versus biogeochemical climate
117 response to historical anthropogenic land cover change, *Geophys. Res. Lett.*, 37,
118 <https://doi.org/10.1029/2010GL043010>, 2010.

119 Popova, S., Utescher, T., Gromyko, D. V., Mosbrugger, V., Herzog, E., and François, L.: Vegetation change in
120 Siberia and the northeast of Russia during the cenozoic cooling: A study based on diversity of plant functional
121 types, *Palaios*, 28, 418–432, <https://doi.org/10.2110/palo.2012.p12-096r>, 2013.

122 Poska, A., Väli, V., Vassiljev, J., Alliksaar, T., and Saarse, L.: Timing and drivers of local to regional scale land-
123 cover changes in the hemiboreal forest zone during the Holocene: A pollen-based study from South Estonia,
124 *Quat. Sci. Rev.*, 277, 107351, <https://doi.org/10.1016/J.QUASCIREV.2021.107351>, 2022.

125 Power, M. J., Marlon, J., Ortiz, N., Bartlein, P. J., Harrison, S. P., Mayle, F. E., Ballouche, A., Bradshaw, R. H.
126 W., Carcaillet, C., Cordova, C., Mooney, S., Moreno, P. I., Prentice, I. C., Thonicke, K., Tinner, W., Whitlock,
127 C., Zhang, Y., Zhao, Y., Ali, A. A., Anderson, R. S., Beer, R., Behling, H., Briles, C., Brown, K. J., Brunelle, A.,
128 Bush, M., Camill, P., Chu, G. Q., Clark, J., Colombaroli, D., Connor, S., Daniau, A. L., Daniels, M., Dodson, J.,
129 Doughty, E., Edwards, M. E., Finsinger, W., Foster, D., Frechette, J., Gaillard, M. J., Gavin, D. G., Gobet, E.,
130 Haberle, S., Hallett, D. J., Higuera, P., Hope, G., Horn, S., Inoue, J., Kaltenrieder, P., Kennedy, L., Kong, Z. C.,
131 Larsen, C., Long, C. J., Lynch, J., Lynch, E. A., McGlone, M., Meeks, S., Mensing, S., Meyer, G., Minckley, T.,

132 Mohr, J., Nelson, D. M., New, J., Newnham, R., Noti, R., Oswald, W., Pierce, J., Richard, P. J. H., Rowe, C.,
133 Sanchez Goñi, M. F., Shuman, B. N., Takahara, H., Toney, J., Turney, C., Urrego-Sanchez, D. H.,
134 Umbanhowar, C., Vandergoes, M., Vanniére, B., Vescovi, E., Walsh, M., Wang, X., Williams, N., Wilmshurst,
135 J., and Zhang, J. H.: Changes in fire regimes since the last glacial maximum: An assessment based on a
136 global synthesis and analysis of charcoal data, *Clim. Dyn.*, 30, 887–907, [https://doi.org/10.1007/S00382-007-](https://doi.org/10.1007/S00382-007-0334-X/FIGURES/5)
137 0334-X/FIGURES/5, 2008.

138 Prentice, I. C., Harrison, S. P., Jolly, D., and Guiot, J.: The climate and biomes of Europe at 6000 yr BP:
139 Comparison of model simulations and pollen-based reconstructions, *Quat. Sci. Rev.*, 17, 659–668,
140 [https://doi.org/10.1016/S0277-3791\(98\)00016-X](https://doi.org/10.1016/S0277-3791(98)00016-X), 1998.

141 Quiquet, A., Roche, D., Dumas, C., Paillard, D., and Roche, D. M.: Online dynamical downscaling of
142 temperature and precipitation within the iLOVECLIM model (version 1.1) Online dynamical downscaling of
143 temperature and precipitation within the iLOVECLIM model (version 1.1). *Geoscientific Model Development*
144 Online dynamical, *Eur. Geosci. Union*, 11, 453–466, <https://doi.org/10.5194/gmd-11-453-2018>, 2018.

145 Ramankutty, N. and Foley, J. A.: Estimating historical changes in global land cover: Croplands from 1700 to
146 1992, *Global Biogeochem. Cycles*, 13, 997–1027, <https://doi.org/10.1029/1999GB900046>, 1999.

147 Raynaud, D., Barnola, J. M., Chappellaz, J., Blunier, T., Indermühle, A., and Stauffer, B.: The ice record of
148 greenhouse gases: a view in the context of future changes, *Quat. Sci. Rev.*, 19, 9–17,
149 [https://doi.org/10.1016/S0277-3791\(99\)00082-7](https://doi.org/10.1016/S0277-3791(99)00082-7), 2000.

150 Ren, Z., Zhu, H., Shi, H., Liu, X., Ren, Z., Zhu, H., Shi, H., and Liu, X.: Shift of potential natural vegetation
151 against global climate change under historical, current and future scenarios, *Rangel. J.*, 43, 309–319,
152 <https://doi.org/10.1071/RJ20092>, 2021.

153 Roberts, C. N., Woodbridge, J., Palmisano, A., Bevan, A., Fyfe, R., and Shennan, S.: Mediterranean
154 landscape change during the Holocene: Synthesis, comparison and regional trends in population, land cover
155 and climate, *Holocene*, 29, 923–937,
156 [https://doi.org/10.1177/0959683619826697/ASSET/IMAGES/LARGE/10.1177_0959683619826697-](https://doi.org/10.1177/0959683619826697/ASSET/IMAGES/LARGE/10.1177_0959683619826697-FIG7.JPEG)
157 FIG7.JPEG, 2019.

158 Roberts, N., Fyfe, R. M., Woodbridge, J., Gaillard, M.-J., Davis, B. A. S. S., Kaplan, J. O., Marquer, L., Mazier,
159 F., Nielsen, A. B., Sugita, S., Trondman, A.-K. K., and Leydet, M.: Europe's lost forests: A pollen-based
160 synthesis for the last 11,000 years, *Sci. Rep.*, 8, 1–8, <https://doi.org/10.1038/s41598-017-18646-7>, 2018.

161 Roberts, P., Buhrich, A., Caetano-Andrade, V., Cosgrove, R., Fairbairn, A., Florin, S. A., Vanwezer, N., Boivin,
162 N., Hunter, B., Mosquito, D., Turpin, G., and Ferrier, Å.: Reimagining the relationship between Gondwanan
163 forests and Aboriginal land management in Australia's "Wet Tropics," *iScience*, 24, 102190,
164 <https://doi.org/10.1016/J.ISCI.2021.102190>, 2021.

165 Roche, D. M.: delta O-18 water isotope in the iLOVECLIM model (version 1.0) - Part 1: Implementation and
166 verification, *Geosci. Model Dev.*, 6, 1481–1491, <https://doi.org/10.5194/gmd-6-1481-2013>, 2013.

167 Roebroeks, W., MacDonald, K., Scherjon, F., Bakels, C., Kindler, L., Nikulina, A., Pop, E., and Gaudzinski-
168 Windheuser, S.: Landscape modification by Last Interglacial Neanderthals, *Sci. Adv.*, 7, 1–14,
169 <https://doi.org/10.1126/sciadv.abj5567>, 2021.

170 Rowley-Conwy, P. and Layton, R.: Foraging and farming as niche construction: stable and unstable
171 adaptations, *Philos. Trans. R. Soc. B Biol. Sci.*, 366, 849–862, <https://doi.org/10.1098/RSTB.2010.0307>, 2011.

172 Ruddiman, W. F.: The Anthropocene, *Annu. Rev. Earth Planet. Sci.*, 41, 45–68,
173 <https://doi.org/10.1146/ANNUREV-EARTH-050212-123944>, 2013.

174 Ruddiman, W. F.: Three flaws in defining a formal 'Anthropocene,' *Prog. Phys. Geogr.*, 42, 451–461,
175 [https://doi.org/10.1177/0309133318783142/ASSET/IMAGES/LARGE/10.1177_0309133318783142-
176 FIG3.JPEG](https://doi.org/10.1177/0309133318783142/ASSET/IMAGES/LARGE/10.1177_0309133318783142-FIG3.JPEG), 2018.

177 Ruddiman, W. F. and Ellis, E. C.: Effect of per-capita land use changes on Holocene forest clearance and CO₂
178 emissions, *Quat. Sci. Rev.*, 28, 3011–3015, <https://doi.org/10.1016/j.quascirev.2009.05.022>, 2009.

179 Ruddiman, W. F., Fuller, D. Q., Kutzbach, J. E., Tzedakis, P. C., Kaplan, J. O., Ellis, E. C., Vavrus, S. J.,
180 Roberts, C. N., Fyfe, R., He, F., Lemmen, C., and Woodbridge, J.: Late Holocene climate: Natural or
181 anthropogenic?, *Rev. Geophys.*, 54, 93–118, <https://doi.org/10.1002/2015RG000503>, 2016.

182 Rull, V.: The "Anthropocene" uncovered, *Collect. Bot.*, 36, <https://doi.org/10.3989/collectbot.2017.v36.008>,
183 2017.

184 Sandom, C. J., Faubry, S., Sandel, B. S., and Svenning, J.-C.: Global late Quaternary megafauna extinctions
185 linked to humans, not climate change, 1–9, <https://doi.org/http://dx.doi.org/10.1098/rspb.2013.3254>, 2014.

186 Scherjon, F., Bakels, C., MacDonald, K., and Roebroeks, W.: Burning the land: An ethnographic study of off-
187 site fire use by current and historically documented foragers and implications for the interpretation of past fire
188 practices in the landscape, *Curr. Anthropol.*, 56, 299–326,
189 <https://doi.org/10.1086/681561/ASSET/IMAGES/LARGE/FG7.JPEG>, 2015.

190 Schilt, A., Baumgartner, M., Blunier, T., Schwander, J., Spahni, R., Fischer, H., and Stocker, T. F.: Glacial-
191 interglacial and millennial-scale variations in the atmospheric nitrous oxide concentration during the last
192 800,000 years, *Quat. Sci. Rev.*, 29, 182–192, <https://doi.org/10.1016/j.quascirev.2009.03.011>, 2010.

193 Seddon, A. W. R., Macias-Fauria, M., and Willis, K. J.: Climate and abrupt vegetation change in Northern
194 Europe since the last deglaciation:, *The Holocene*, 25, 25–36, <https://doi.org/10.1177/0959683614556383>,
195 2014.

196 Serge, M. A.: Spatially extensive and temporally continuous three REVEALS pollen-based vegetation
197 reconstructions in Europe over the Holocene, data.InDoRES, V1, 2023.

198 Serge, M. A., Mazier, F., Fyfe, R., Gaillard, M.-J., Klein, T., Lagnoux, A., Galop, D., Githumbi, E., Mindrescu,
199 M., Nielsen, A. B., Trondman, A.-K., Poska, A., Sugita, S., and Woodbridge, J.: Testing the Effect of Relative
200 Pollen Productivity on the REVEALS Model: A Validated Reconstruction of Europe-Wide Holocene Vegetation,
201 *L.* 2023, Vol. 12, Page 986, 12, 986, <https://doi.org/10.3390/LAND12050986>, 2023.

202 Shennan, S., Downey, S. S., Timpson, A., Edinborough, K., Colledge, S., Kerig, T., Manning, K., and Thomas,
203 M. G.: Regional population collapse followed initial agriculture booms in mid-Holocene Europe, *Nat. Commun.*
204 2013 41, 4, 1–8, <https://doi.org/10.1038/ncomms3486>, 2013.

205 Smith, B. D. and Zeder, M. A.: The onset of the Anthropocene, *Anthropocene*, 4, 8–13,
206 <https://doi.org/10.1016/J.ANCENE.2013.05.001>, 2013.

207 Smith, M. C., Singarayer, J. S., Valdes, P. J., Kaplan, J. O., and Branch, N. P.: The biogeophysical climatic
208 impacts of anthropogenic land use change during the Holocene, *Clim. Past*, 12, 923–941,
209 <https://doi.org/10.5194/cp-12-923-2016>, 2016.

210 Somodi, I., Molnár, Z., and Ewald, J.: Towards a more transparent use of the potential natural vegetation
211 concept – an answer to Chiarucci et al., *J. Veg. Sci.*, 23, 590–595, <https://doi.org/10.1111/J.1654->
212 [1103.2011.01378.X](https://doi.org/10.1111/J.1654-1103.2011.01378.X), 2012.

213 Steffen, W., Grinevald, J., Crutzen, P., and McNeill, J.: The Anthropocene: conceptual and historical
214 perspectives, *Philos. Trans. R. Soc. A Math. Phys. Eng. Sci.*, 369, 842–867,
215 <https://doi.org/10.1098/RSTA.2010.0327>, 2011.

216 Stephens, L., Fuller, D., Boivin, N., Rick, T., Gauthier, N., Kay, A., Marwick, B., Armstrong, C. G. D., Barton, C.
217 M., Denham, T., Douglass, K., Driver, J., Janz, L., Roberts, P., Rogers, J. D., Thakar, H., Johnson, A. L.,
218 Vattuone, M. M. S., Aldenderfer, M., Archila, S., Artioli, G., Bale, M. T., Beach, T., Borrell, F., Braje, T.,
219 Buckland, P. I., Cano, N. G. J., Capriles, J. M., Castillo, A. D., Çilingiroğlu, Ç., Cleary, M. N., Conolly, J.,
220 Coutros, P. R., Covey, R. A., Cremaschi, M., Crowther, A., Der, L., di Lernia, S., Doershuk, J. F., Doolittle, W.
221 E., Edwards, K. J., Erlandson, J. M., Evans, D., Fairbairn, A., Faulkner, P., Feinman, G., Fernandes, R.,
222 Fitzpatrick, S. M., Fyfe, R., Garcea, E., Goldstein, S., Goodman, R. C., Guedes, J. D., Herrmann, J., Hiscock,
223 P., Hommel, P., Horsburgh, K. A., Hritz, C., Ives, J. W., Junno, A., Kahn, J. G., Kaufman, B., Kearns, C.,
224 Kidder, T. R., Lanoë, F., Lawrence, D., Lee, G. A., Levin, M. J., Lindsoug, H. B., López-Sáez, J. A., Macrae,
225 S., Marchant, R., Marston, J. M., McClure, S., McCoy, M. D., Miller, A. V., Morrison, M., Matuzeviciute, G. M.,
226 Müller, J., Nayak, A., Noerwidi, S., Peres, T. M., Peterson, C. E., Proctor, L., Randall, A. R., Renette, S.,
227 Schug, G. R., Ryzewski, K., Saini, R., Scheinsohn, V., Schmidt, P., Sebillaud, P., Simpson, I. A., Softysiak, A.,
228 Speakman, R. J., Spengler, R. N., Steffen, M. L., Storzum, M. J., Strickland, K. M., et al.: Archaeological
229 assessment reveals Earth’s early transformation through land use, *Science (80-.)*, 365, 897–902,
230 <https://doi.org/https://doi.org/10.1126/science.aax1192>, 2019.

231 Stewart, M., Carleton, W. C., and Groucutt, H. S.: Climate change, not human population growth, correlates
232 with Late Quaternary megafauna declines in North America, *Nat. Commun.*, 12, 1–15,
233 <https://doi.org/10.1038/s41467-021-21201-8>, 2021.

234 Stocker, B. D., Strassmann, K., and Joos, F.: Sensitivity of Holocene atmospheric CO₂ and the modern
235 carbon budget to early human land use: analyses with a process-based model, *Biogeosciences*, 8, 69–88,
236 <https://doi.org/10.5194/bg-8-69-2011>, 2011.

237 Strandberg, G., Lindström, J., Poska, A., Zhang, Q., Fyfe, R., Githumbi, E., Kjellström, E., Mazier, F., Nielsen,
238 A. B., Sugita, S., Trondman, A. K., Woodbridge, J., and Gaillard, M. J.: Mid-Holocene European climate
239 revisited: New high-resolution regional climate model simulations using pollen-based land-cover, *Quat. Sci.*
240 *Rev.*, 281, 107431, <https://doi.org/10.1016/J.QUASCIREV.2022.107431>, 2022.

241 Strona, G., Mauri, A., Veech, J. A., Seufert, G., Ayanz, J. S. M., and Fattorini, S.: Far from Naturalness: How
242 Much Does Spatial Ecological Structure of European Tree Assemblages Depart from Potential Natural
243 Vegetation?, *PLoS One*, 11, e0165178, <https://doi.org/10.1371/JOURNAL.PONE.0165178>, 2016.

244 Stuart, A. and Ord, J. K.: Kendall's Advanced Theory of Statistics, Distribution theory, *Sci. Res. Publ.*, 1, 1994.

245 Sugita, S.: Theory of quantitative reconstruction of vegetation I: pollen from large sites REVEALS regional
246 vegetation composition., <http://dx.doi.org/10.1177/0959683607075837>, 17, 229–241,
247 <https://doi.org/10.1177/0959683607075837>, 2007.

248 Sun, Y., Xu, Q., Gaillard, M. J., Zhang, S., Li, D., Li, M., Li, Y., Li, X., and Xiao, J.: Pollen-based reconstruction
249 of total land-cover change over the Holocene in the temperate steppe region of China: An attempt to quantify
250 the cover of vegetation and bare ground in the past using a novel approach, *CATENA*, 214, 106307,
251 <https://doi.org/10.1016/J.CATENA.2022.106307>, 2022.

252 Swindles, G. T., Roland, T. P., and Ruffell, A.: The 'Anthropocene' is most useful as an informal concept, *J.*
253 *Quat. Sci.*, 38, 453–454, <https://doi.org/10.1002/JQS.3492>, 2023.

254 Tarasov, L. and Peltier, W. R.: Greenland glacial history and local geodynamic consequences, *Geophys. J.*
255 *Int.*, 150, 198–229, <https://doi.org/10.1046/J.1365-246X.2002.01702.X/2/150-1-198-FIG015.JPEG>, 2002.

256 Tarasov, L., Dyke, A. S., Neal, R. M., and Peltier, W. R.: A data-calibrated distribution of deglacial chronologies
257 for the North American ice complex from glaciological modeling, *Earth Planet. Sci. Lett.*, 315–316, 30–40,
258 <https://doi.org/10.1016/J.EPSL.2011.09.010>, 2012.

259 Trondman, A.-K. K., Gaillard, M.-J., Mazier, F., Sugita, S., Fyfe, R., Nielsen, A. B., Twiddle, C., Barratt, P.,
260 Birks, H. J. B., Bjune, A. E., Björkman, L., Broström, A., Caseldine, C., David, R., Dodson, J., Dörfler, W.,
261 Fischer, E., van Geel, B., Giesecke, T., Hultberg, T., Kalnina, L., Kangur, M., van der Knaap, P., Koff, T.,
262 Kuneš, P., Lagerås, P., Latalowa, M., Lechterbeck, J., Leroyer, C., Leydet, M., Lindbladh, M., Marquer, L.,

263 Mitchell, F. J. G. G., Odgaard, B. V., Peglar, S. M., Persson, T., Poska, A., Rösch, M., Seppä, H., Veski, S.,
264 Wick, L., Latalowa, M., Lechterbeck, J., Leroyer, C., Leydet, M., Lindbladh, M., Marquer, L., Mitchell, F. J. G.
265 G., Odgaard, B. V., Peglar, S. M., Persson, T., Poska, A., Rösch, M., Seppä, H., Veski, S., and Wick, L.:
266 Pollen-based quantitative reconstructions of Holocene regional vegetation cover (plant-functional types and
267 land-cover types) in Europe suitable for climate modelling, *Glob. Chang. Biol.*, 21, 676–697,
268 <https://doi.org/10.1111/gcb.12737>, 2015.

269 Vanni re, B., Blarquez, O., Rius, D., Doyen, E., Br ucher, T., Colombaroli, D., Connor, S., Feurdean, A.,
270 Hickler, T., Kaltenrieder, P., Lemmen, C., Leys, B., Massa, C., and Olofsson, J.: 7000-year human legacy of
271 elevation-dependent European fire regimes, *Quat. Sci. Rev.*, 132, 206–212, 2016.

272 Vavrus, S. J., Kucharik, C. J., He, F., Kutzbach, J. E., and Ruddiman, W. F.: Did agriculture beget agriculture
273 during the past several millennia?, *Holocene*, 32, 680–689,
274 https://doi.org/10.1177/09596836221088231/ASSET/IMAGES/LARGE/10.1177_09596836221088231-
275 [FIG2.JPEG](https://doi.org/10.1177/09596836221088231/ASSET/IMAGES/LARGE/10.1177_09596836221088231-FIG2.JPEG), 2022.

276 Vrac, M.: Multivariate bias adjustment of high-dimensional climate simulations: The Rank Resampling for
277 Distributions and Dependences (R2D2) bias correction, *Hydrol. Earth Syst. Sci.*, 22, 3175–3196,
278 <https://doi.org/10.5194/hess-22-3175-2018>, 2018.

279 Vrac, M., Drobinski, P., Merlo, A., Herrmann, M., Lavaysse, C., Li, L., and Somot, S.: Dynamical and statistical
280 downscaling of the French Mediterranean climate: Uncertainty assessment, *Nat. Hazards Earth Syst. Sci.*, 12,
281 2769–2784, <https://doi.org/10.5194/nhess-12-2769-2012>, 2012.

282 Warnant, P., Fran ois, L. M., Strivay, D., and G rard, J. -C: CARAIB: A global model of terrestrial biological
283 productivity, *Global Biogeochem. Cycles*, 8, 255–270, <https://doi.org/10.1029/94GB00850>, 1994.

284 Waters, C. N., Zalasiewicz, J., Summerhayes, C., Barnosky, A. D., Poirier, C., Ga uszka, A., Cearreta, A.,
285 Edgeworth, M., Ellis, E. C., Ellis, M., Jeandel, C., Leinfelder, R., McNeill, J. R., Richter, D. D. B., Steffen, W.,
286 Syvitski, J., Vidas, D., Wagreich, M., Williams, M., Zhisheng, A., Grinevald, J., Odada, E., Oreskes, N., and
287 Wolfe, A. P.: The Anthropocene is functionally and stratigraphically distinct from the Holocene, *Science (80-.)*,
288 351, aad2622–aad2622, <https://doi.org/10.1126/science.aad2622>, 2016.

289 Williams, M., Zalasiewicz, J., Haff, P. K., Schwägerl, C., Barnosky, A. D., and Ellis, E. C.: The anthropocene
290 biosphere, <https://doi.org/10.1177/2053019615591020>, 18 December 2015.

291 Woodbridge, J., Fyfe, R., Roberts, C., Trondman, A., Mazier, F., and Davis, B.: European forest cover since
292 the start of Neolithic agriculture: a critical comparison of pollen-based reconstructions, *Past Glob. Chang.*
293 *Mag.*, 26, 10–11, <https://doi.org/10.22498/pages.26.1.10>, 2018.

294 Zalasiewicz, J., Waters, C. N., Ellis, E. C., Head, M. J., Vidas, D., Steffen, W., Thomas, J. A., Horn, E.,
295 Summerhayes, C. P., Leinfelder, R., McNeill, J. R., Gałuszka, A., Williams, M., Barnosky, A. D., Richter, D. de
296 B., Gibbard, P. L., Syvitski, J., Jeandel, C., Cearreta, A., Cundy, A. B., Fairchild, I. J., Rose, N. L., Sul, J. A. I.
297 do, Shotyk, W., Turner, S., Wagnreich, M., and Zinke, J.: The Anthropocene: Comparing Its Meaning in Geology
298 (Chronostratigraphy) with Conceptual Approaches Arising in Other Disciplines, *Earth's Futur.*, 9,
299 e2020EF001896, <https://doi.org/10.1029/2020EF001896>, 2021.

300 Zapolska, A., Vrac, M., Quiquet, A., Extier, T., Arthur, F., Renssen, H., and Roche, D. M.: Improving biome and
301 climate modelling for a set of past climate conditions: evaluating bias correction using the CDF-t approach,
302 *Environ. Res. Clim.*, 2, 025004, <https://doi.org/10.1088/2752-5295/ACCBE2>, 2023.

303 Zhang, Y., Renssen, H., Seppä, H., and Valdes, P. J.: Holocene temperature evolution in the Northern
304 Hemisphere high latitudes – Model-data comparisons, *Quat. Sci. Rev.*, 173, 101–113,
305 <https://doi.org/10.1016/j.quascirev.2017.07.018>, 2017.

306

307 Supplementary material

308

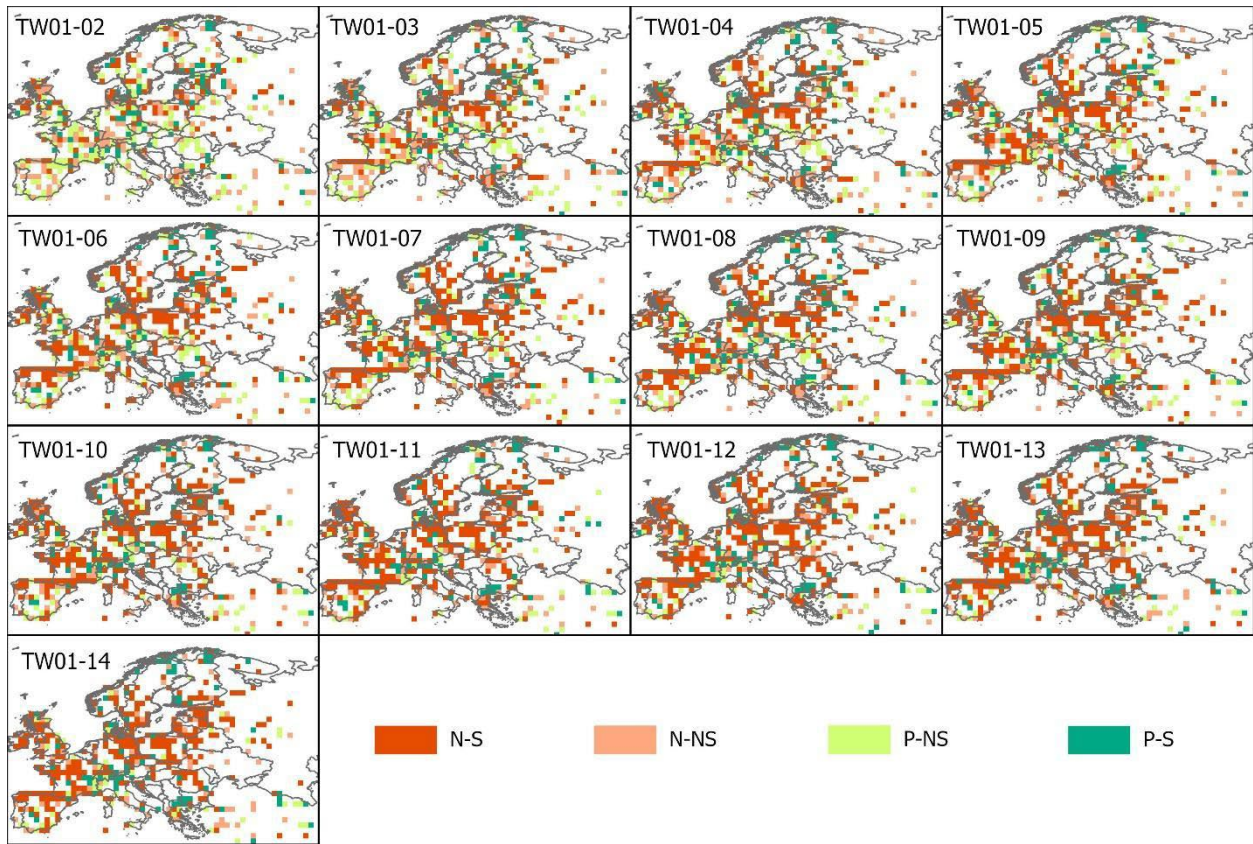
TW	Age range cal BP	TW length(years)
1	AD 2015-1850	165
2	100-350 BP	250
3	350-700 BP	350
4	700-1200 BP	500
5	1200-1700 BP	500
6	1700-2200 BP	500
7	2200-2700 BP	500
8	2700-3200 BP	500
9	3200-3700 BP	500
10	3700-4200 BP	500
11	4200-4700 BP	500
12	4700-5200 BP	500
13	5200-5700 BP	500
14	5700-6200 BP	500

309 Supplementary table 1. Definition of time windows used in this study.

310

311

312



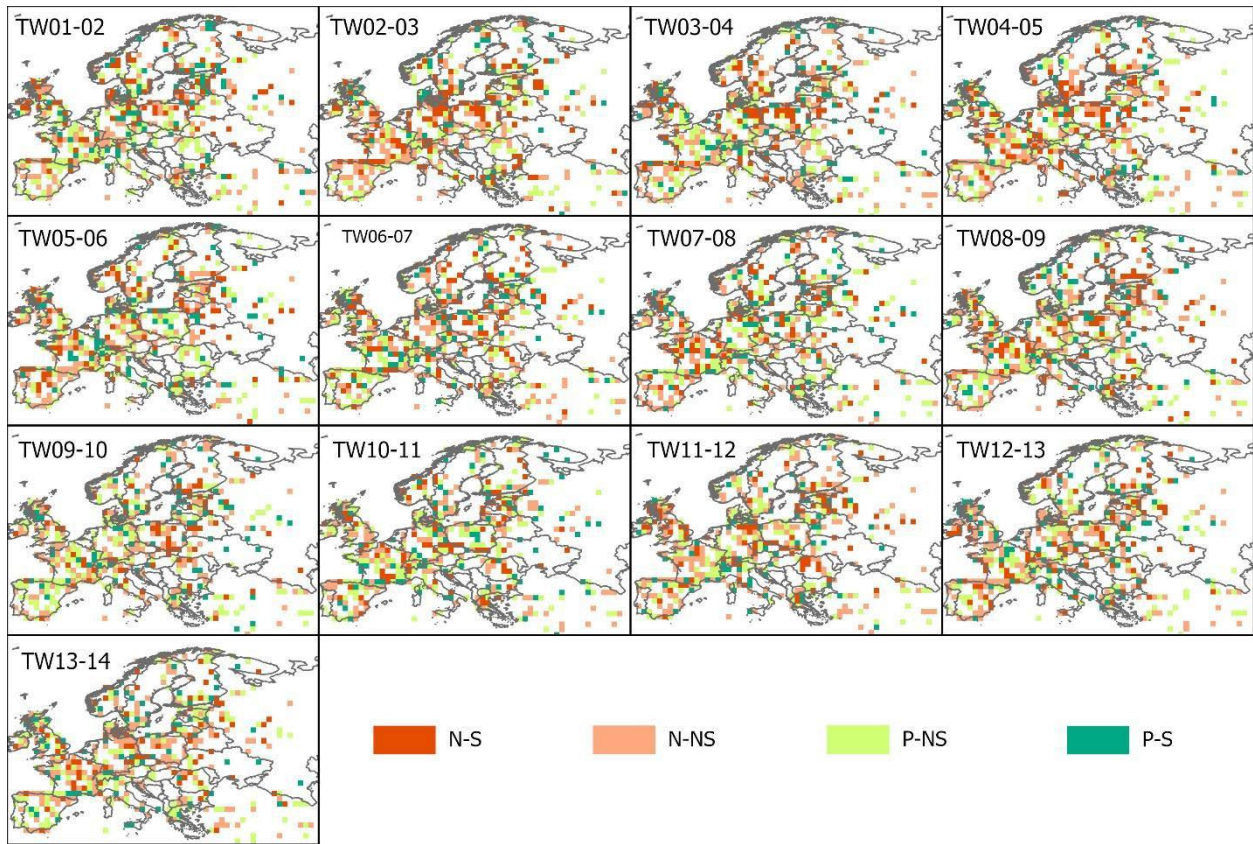
313

314

315 Supplementary figure 1. Difference in WMR between the TW1 (present -100 BP) and each consequent TW. P:
 316 positive slope (more recent time window has lower WMR/ higher human pressure index); N: negative slope
 317 (more recent time window has higher WMR/lower human pressure index); S: significant; NS: non-significant.

318

319



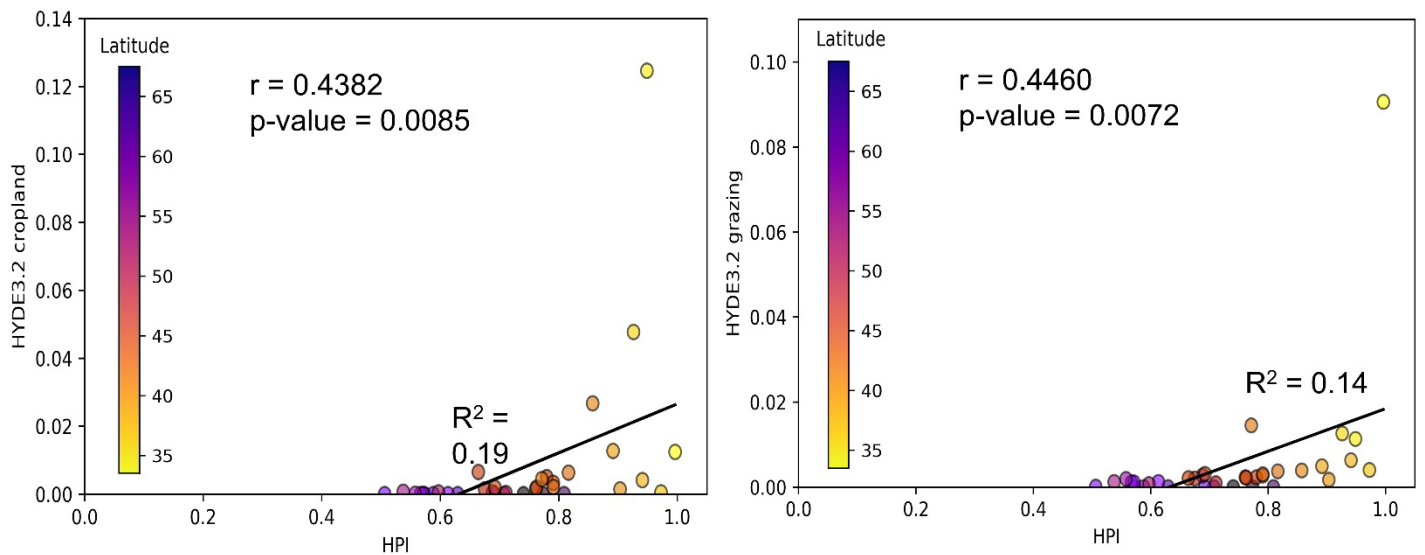
320

321

322

323

Supplementary figure 2. Difference in WMR between the two neighbouring TWs. P: positive slope (more recent time window has lower WMR/ higher human pressure index); N: negative slope (more recent time window has higher WMR/lower human pressure index); S: significant; NS: non-significant.



324

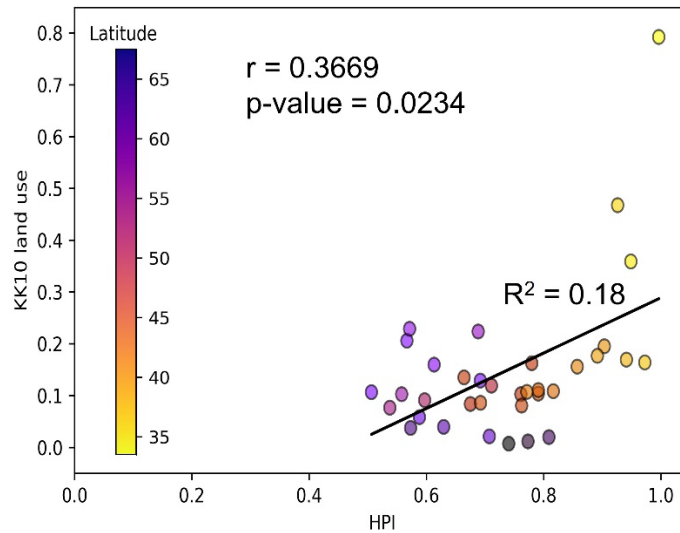
325

326

327

Supplementary Figure 3. Comparison of human pressure index (HPI) versus HYDE 3.2 simulated cropland estimates (left panel) and HYDE 3.2 simulated grazing (right panel), expressed as fraction of croplands and grazing over latitudinal zones in Europe for TW14 (5700-6200 BP).

328



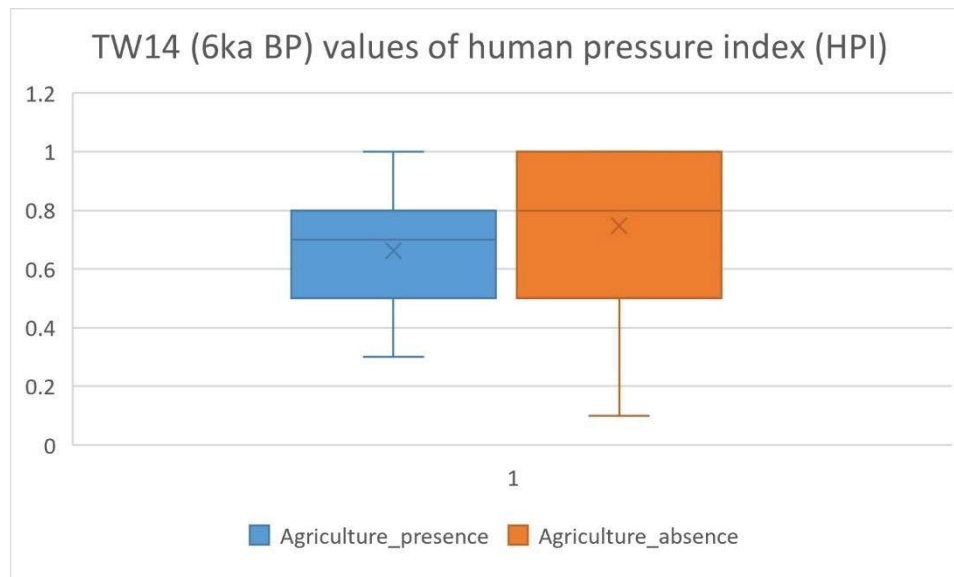
329

330

Supplementary Figure 4. Comparison of human pressure index (HPI) versus KK10 simulated land use,

331

expressed as fraction of croplands and grazing over latitudinal zones in Europe for TW14 (5700-6200 BP).



332

333

Supplementary Figure 5. Human pressure index (HPI) values of grid cells with (blue) and without (orange) the

334

presence of agricultural taxa in REVEALS estimates, represented by *Cerealia t.* and *Secale cereale* pollen at

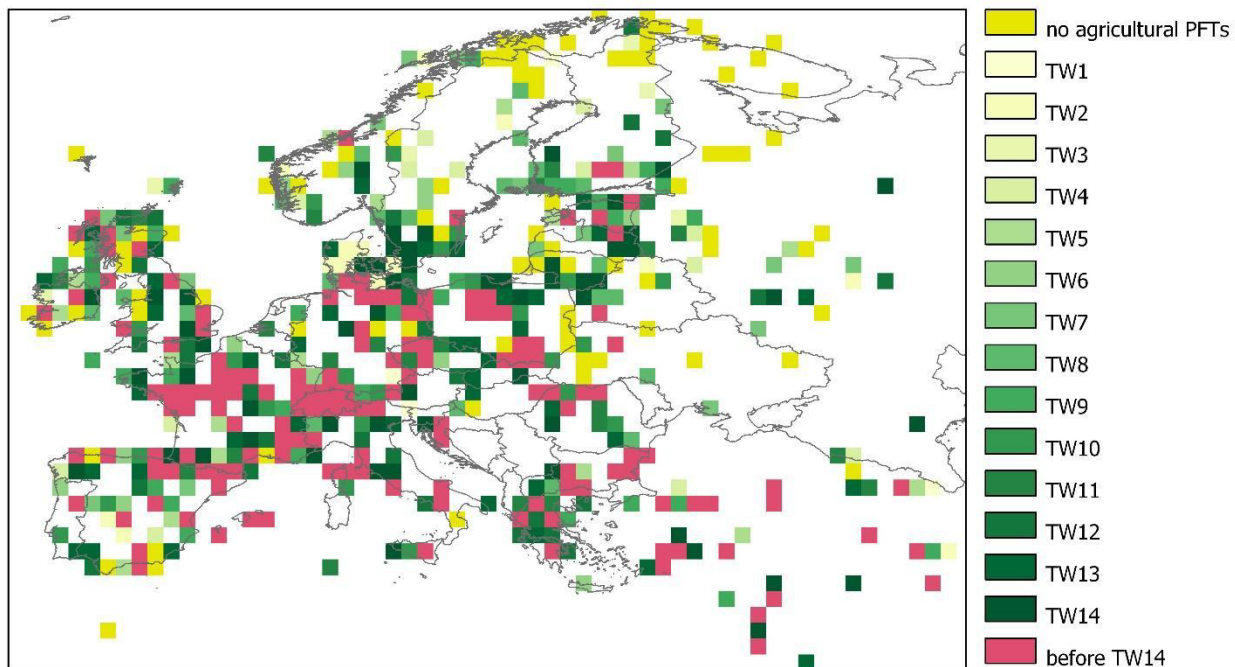
335

TW14 (5700-6200 BP).

336

337

338

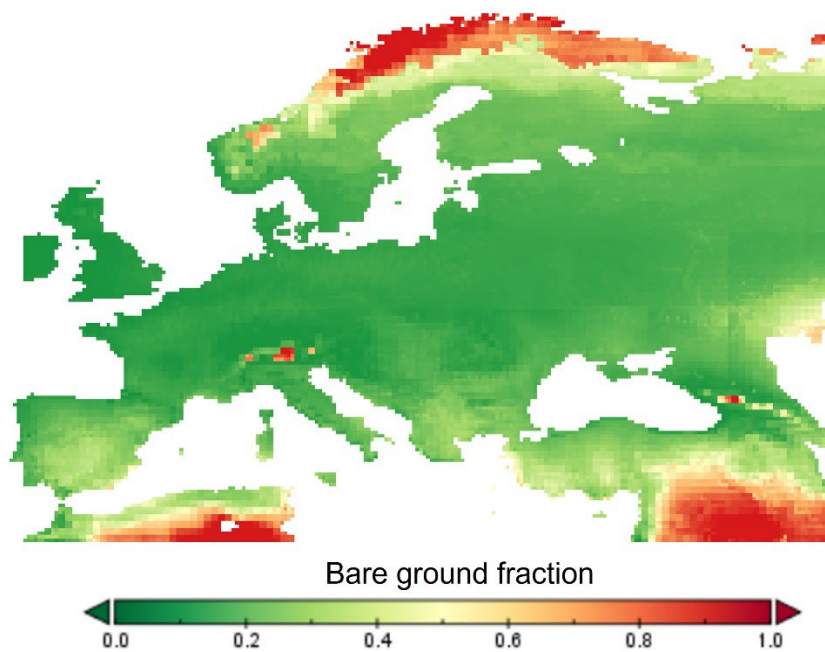


339

340

341

Supplementary Figure 6. Agricultural onset in REVEALS vegetation reconstructions, marked by first appearance of *Cerealia t.* and *Secale cereale* pollen in the dataset.



342

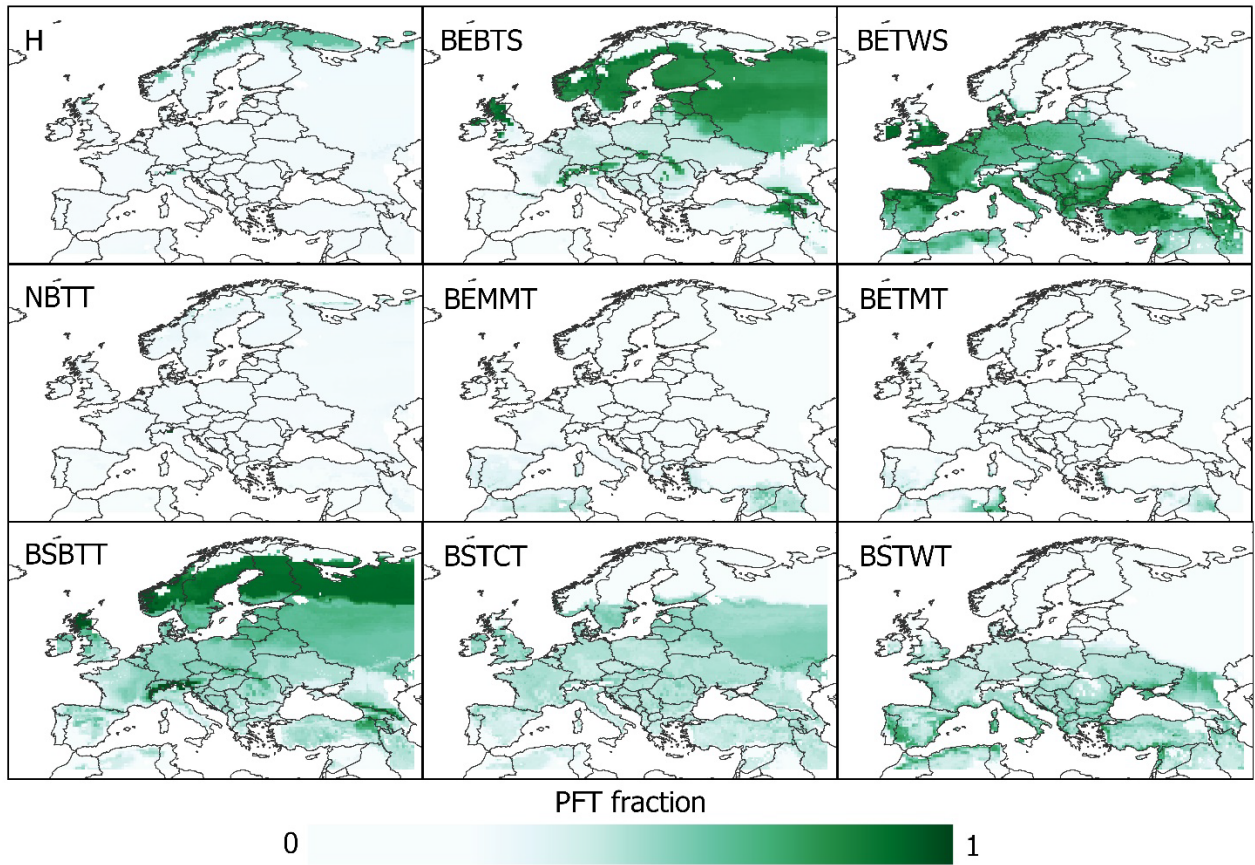
343

344

345

346

Supplementary Figure 7. Fraction of bare ground simulated by CARAIB at TW14 (5700-6200 BP). Due to the similarities observed among all studied TWs, the plotting of other TWs was omitted. The presented pattern of bare ground distribution can be considered representative for all TWs included in the current study.



347

348

349

350

351

Supplementary Figure 8. Fraction of each of the analysed plant functional types at the starting point of our analysis (TW14; 5700-6200 BP), modelled by CARAIB vegetation model. The data for all TWs is provided as a supplementary dataset to this article.